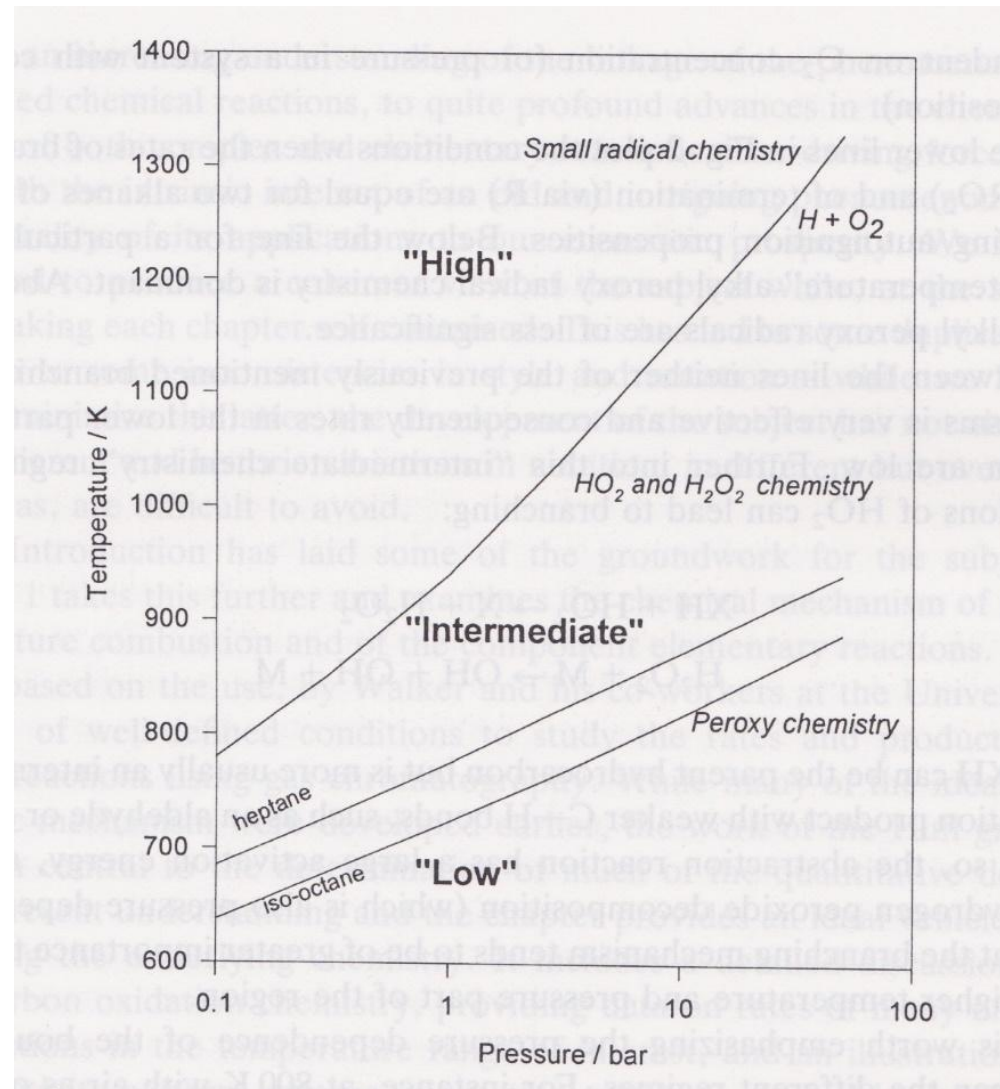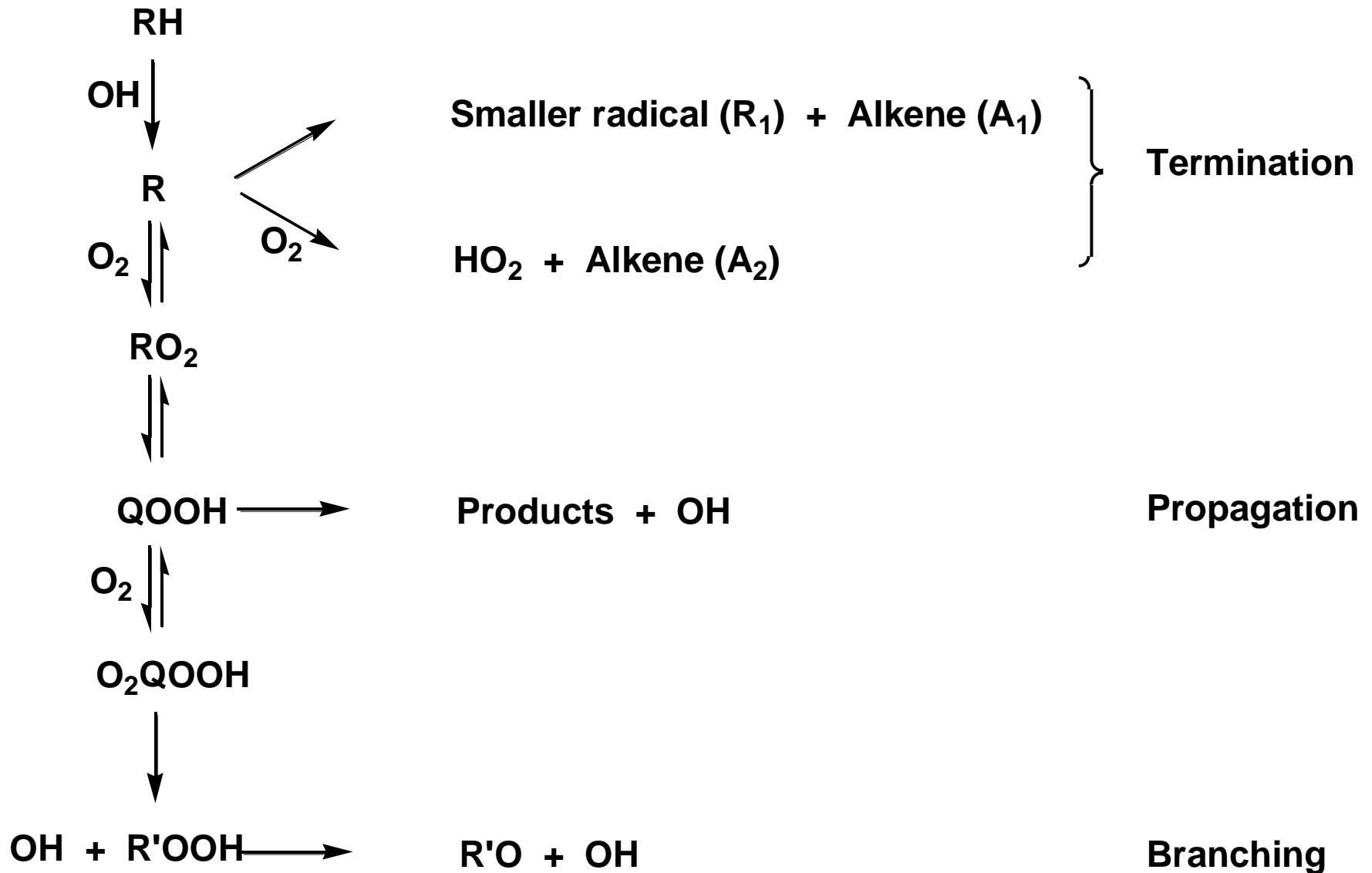# Topic 7
## Peroxy radical chemistry and autoignition

Low temperature combustion

- Combustion in the 500 – 1000 K range shows regions of slow reaction and regions of explosion or ignition.
- Cause of 'knock' in gasoline engine and of the desired autoignition in diesel engines
- There is a region of "negative temperature coefficient", where the reaction changes from branching to termination as T increases, in the boundary between low temperature and high temperature combustion
- Peroxy radical chemistry is central to combustion in the low temperature regime
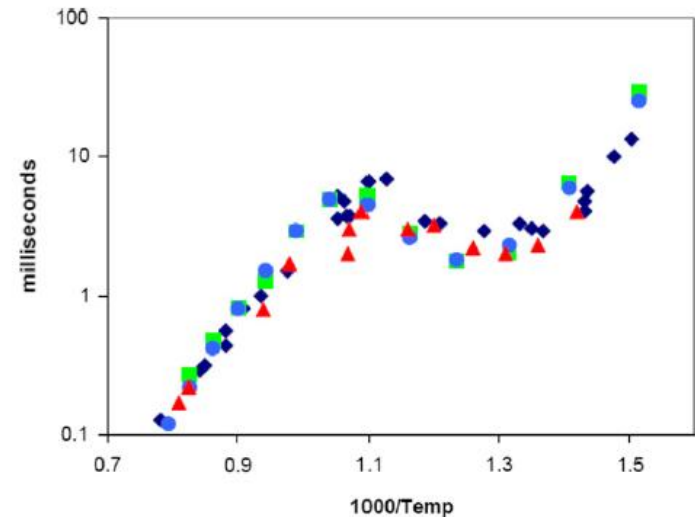
Autoignition chemistry

RH

OH ↓

R → **Smaller radical (R$_1$) + Alkene (A$_1$)**

O$_2$ ⇅   →$_{O_2}$ **HO$_2$ + Alkene (A$_2$)**

} **Termination**

RO$_2$

⇅

QOOH ⟶ **Products + OH**   **Propagation**

O$_2$ ⇅

O$_2$QOOH

↓

OH + R'OOH ⟶ **R'O + OH**   **Branching**

Negative temperature coefficient
Westbrook et al, Comb and Flame, 156(2009) 181
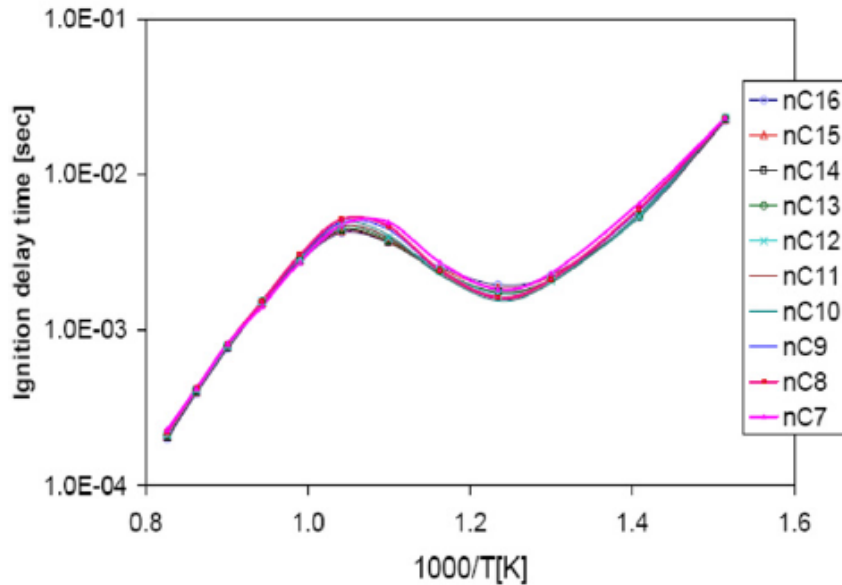
Computed ignition delay times for stoichiometric n-alkanes in air at 13.5 bar.

- Shock tube ignition delay times for n-heptane and n-decane, all at 13.5 bar pressure and stoichiometric fuel/air. Experiments are n-heptane (diamond) and n-decane (Triangle) n-Heptane (square) Computed results n-decane (circle)

Static reactors: Early studies of alkane oxidation kinetics and mechanism by Baldwin, Walker and co-workers

- The techniques rely on end product analysis using gas chromatography. Three techniques were used:
  - Addition of small amounts of alkane, RH, to a slowly reacting $H_{2\,+}\,O_2$ mixture at ~ 750 K allowed measurements of, e.g. OH, H, HO_2 + RH. $H_2 + O_2$ provides a well-controlled environment containing the radicals. (JCS Faraday Trans 1., 1975, 71, 736)
  - Oxidation of aldehydes (550 – 800 K). Aldehydes act as a source of alkyl radicals, e.g. $2\text{-}C_3H_7$ from $2\text{-}C_3H_7CHO$ (JCS Faraday Trans 2., 1987, 83, 1509)
  - Decomposition of tetramethylbutane (TMB) in the prsence of O_2. System acts as a source of $HO_{2.}$ (JCS Faraday Trans 1., 1986, 82, 89)

Whole system studies
Provide targets for mechanism evaluation

Flow reactor study of dimethyl ether oxidation at low T
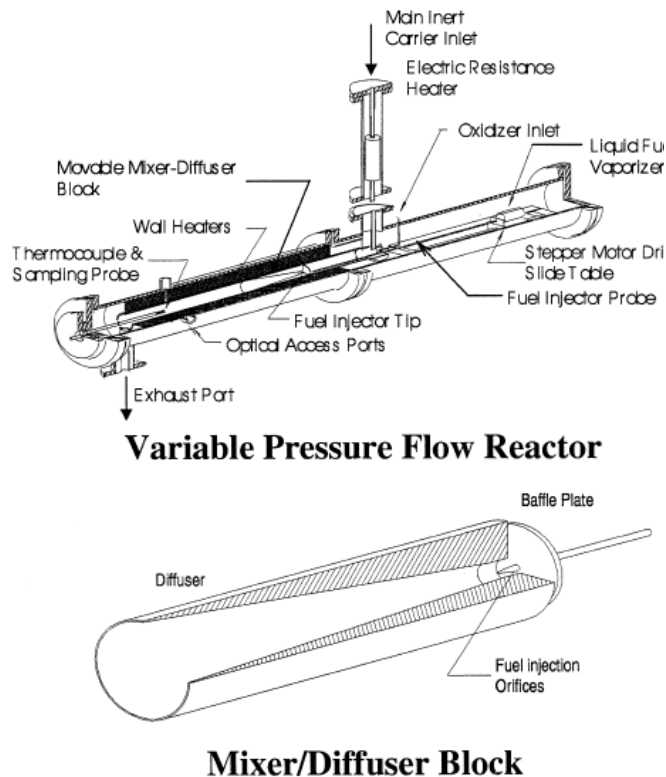## Fischer et al. Int J Chem Kinet (32, 741, 2000)

Variable Pressure Flow Reactor

Mixer/Diffuser Block

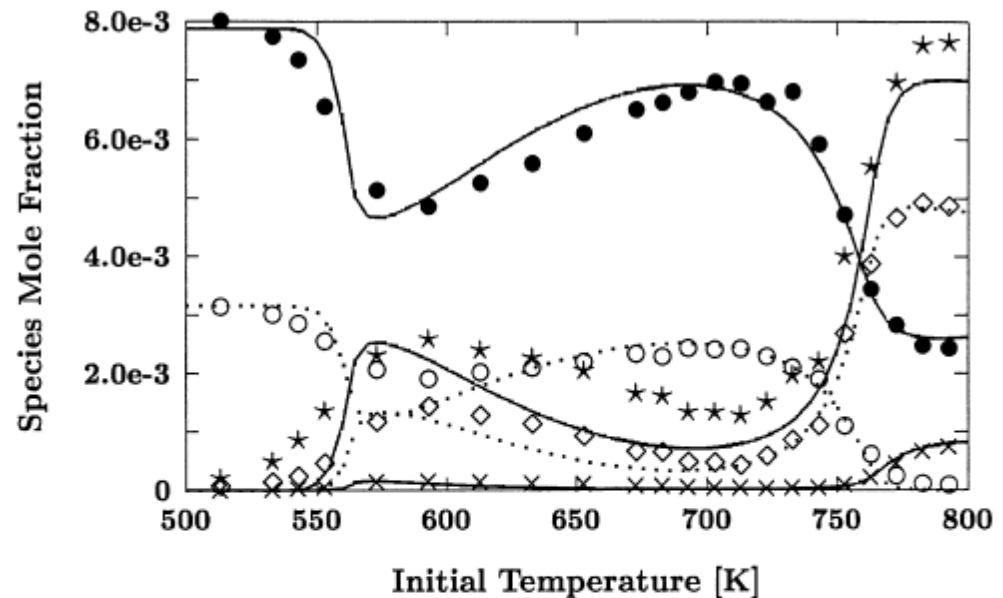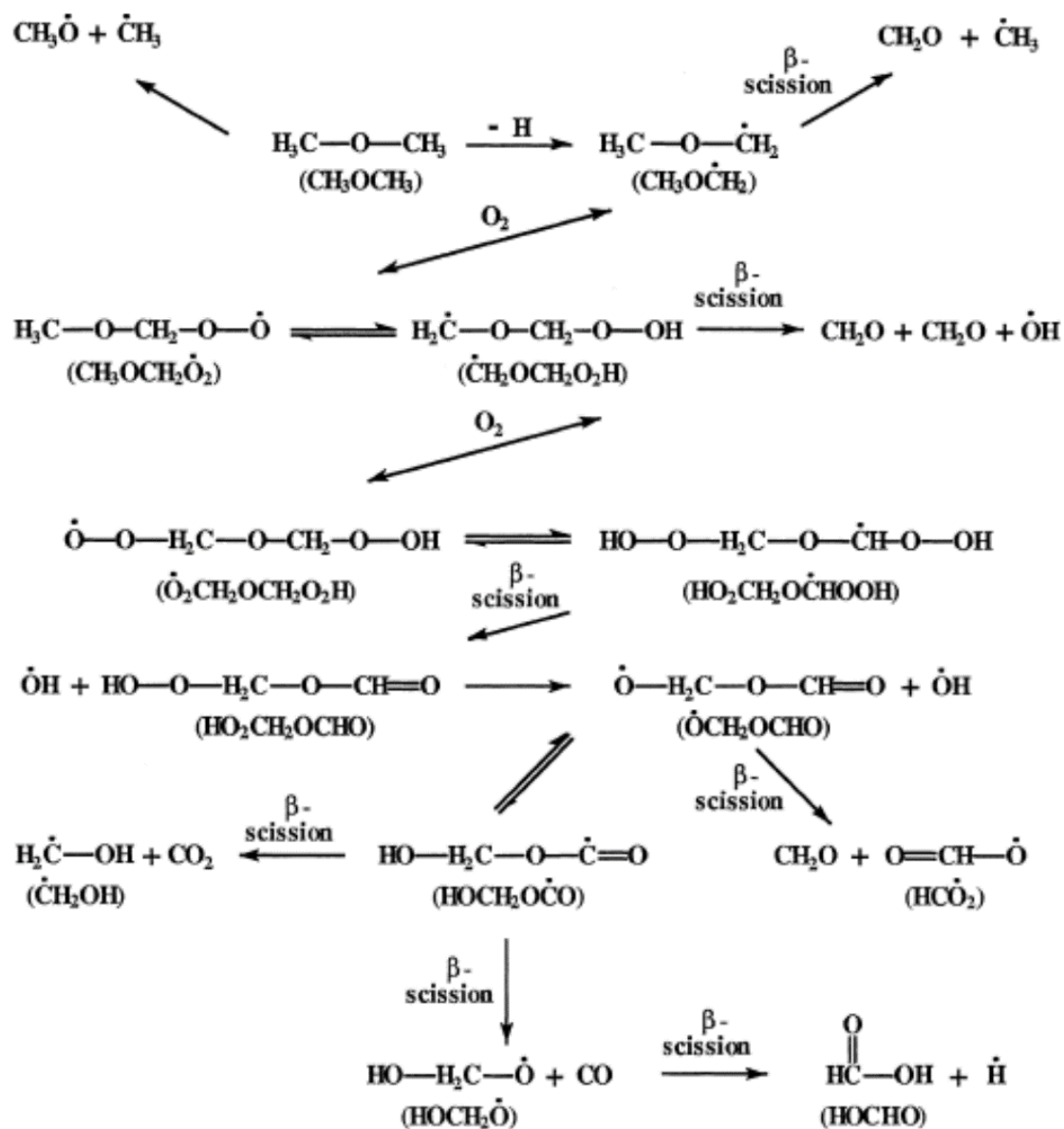**Figure 1** Princeton variable-pressure flow reactor mixer block assembly.

Figure 3 Measured (symbols) and calculated (curves) species concentrations from a flow reactor. 3030 ppm DME, $\phi = 1.19$, $P = 12.5$ atm, $\tau = 1.8$ s. ● O_2, ○ CH_3OCH_3, ★ H_2O, ◇ CO, and × CO_2. Dotted lines correspond to open symbols.

- 550–850 K, 12–18 atm, at equivalence ratios of 0.7 - 4.2
- FTIR, non-dispersive IR (NDIR) (for CO and CO_2), and electrochemical (for O_2)
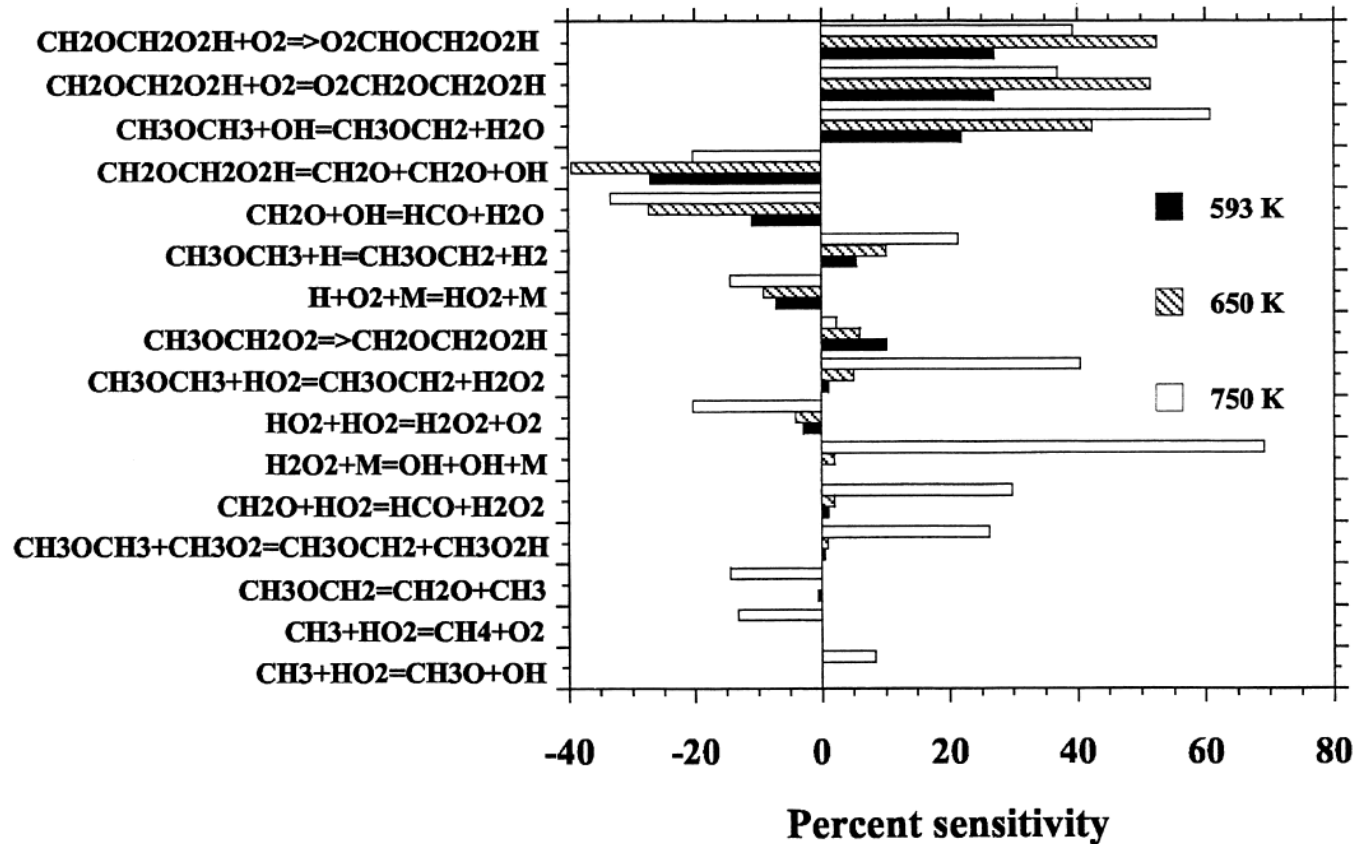
Mechanism

Sensitivity analysis

CH2OCH2O2H+O2=>O2CHOCH2O2H
CH2OCH2O2H+O2=O2CH2OCH2O2H
CH3OCH3+OH=CH3OCH2+H2O
CH2OCH2O2H=CH2O+CH2O+OH
CH2O+OH=HCO+H2O
CH3OCH3+H=CH3OCH2+H2
H+O2+M=HO2+M
CH3OCH2O2=>CH2OCH2O2H
CH3OCH3+HO2=CH3OCH2+H2O2
HO2+HO2=H2O2+O2
H2O2+M=OH+OH+M
CH2O+HO2=HCO+H2O2
CH3OCH3+CH3O2=CH3OCH2+CH3O2H
CH3OCH2=CH2O+CH3
CH3+HO2=CH4+O2
CH3+HO2=CH3O+OH

■ 593 K
▨ 650 K
□ 750 K

-40   -20   0   20   40   60   80

Percent sensitivity

Figure 28 Sensitivity coefficients for dimethyl ether oxidation. 3030 ppm DME, ϕ = 1.19, P = 12.5 atm, τ = 2.1 s.

- See also Fischer et al. Int J Chem Kinet (32, 713, 2000) for a study at higher T (2.5 atm, 1118 K) using the same technique
- Other methods used: Jet Stirred reactor (Proc Comb Inst, 1996, 23, 627).

Jet stirred reactor, coupled with synchrotron vacuum ultraviolet photoionization molecular-beam mass spectrometry
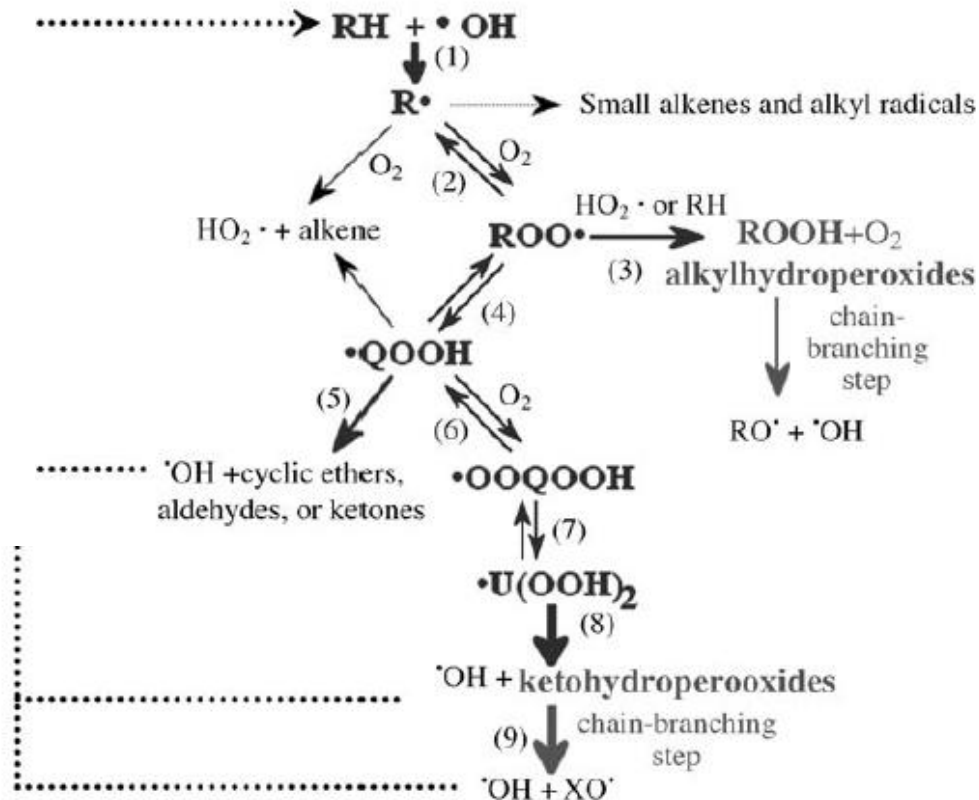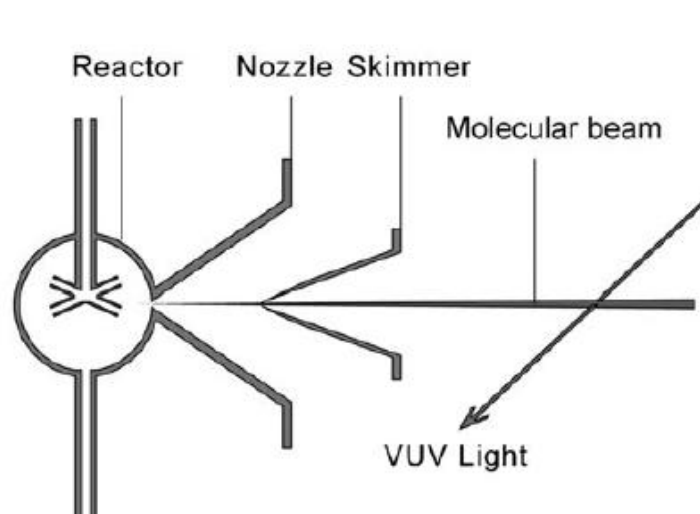
- Provided direct observation of speciated hydroperoxides for the first time

Experimental and modelling observations, oxidation of n-butane

Mass spectrum, 590 K, photon energy 10.0 ev
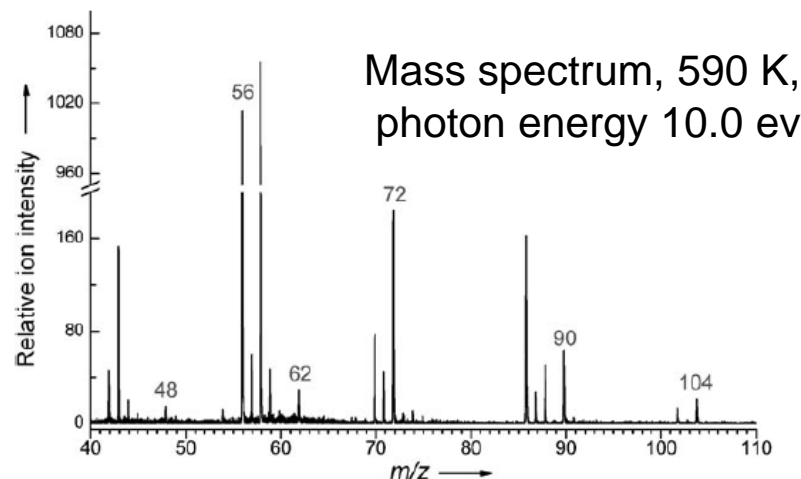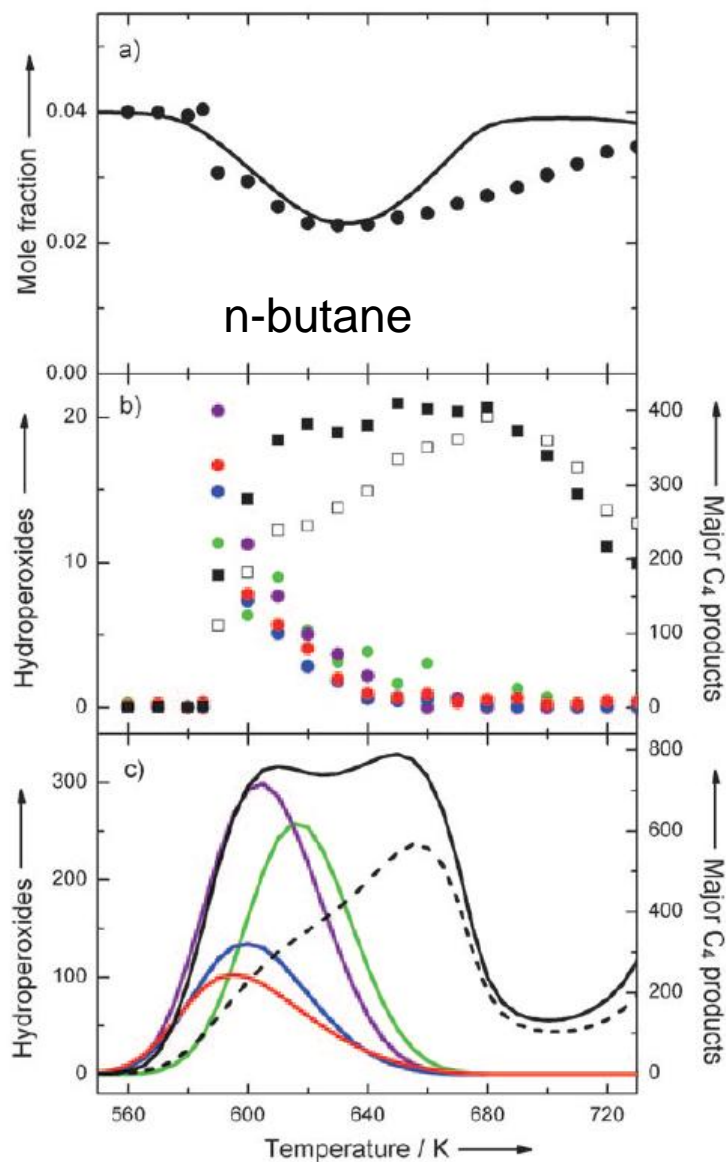
- **Experiment:** m/z 48 (green circles), 56 (white squares, the signal is divided by 7.5), 62 (purple circles), 72 (black squares), 90 (blue circles, the signal is divided by 4) and 104 (red circles)

- **Calculated:** (ppm) CH_3OOH (48) (green line, mole fraction divided by 5), C_2H_5OOH (62) (purple line), C_4H_9OOH (90) (blue line), the C4 ketohydroperoxides (104) (red line), butenes (56) (dash line, mole fraction divided by 5), and C_4H_8O products (72) (black line)

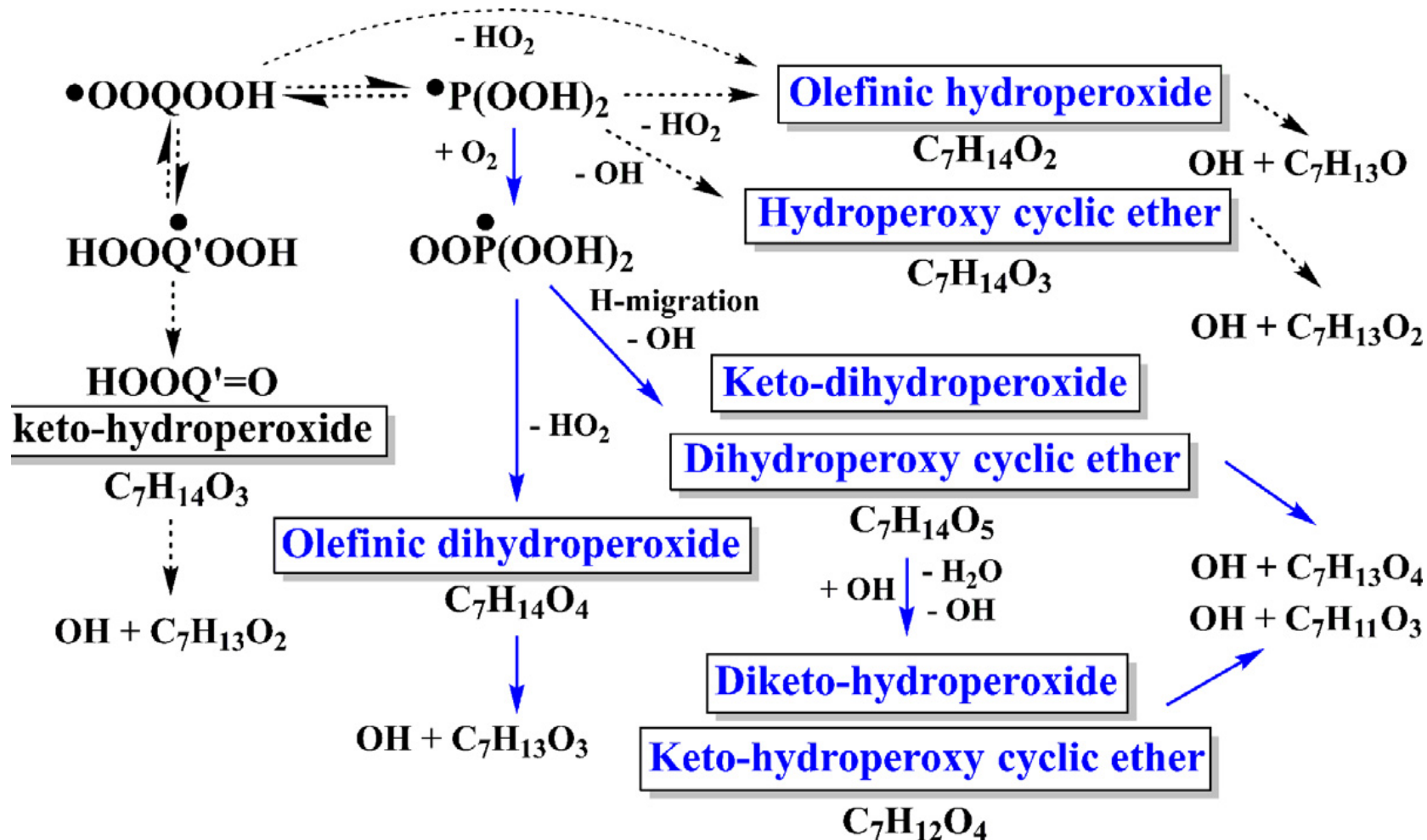# Evidence for a third O_2 addition in 2-methylhexane combustion
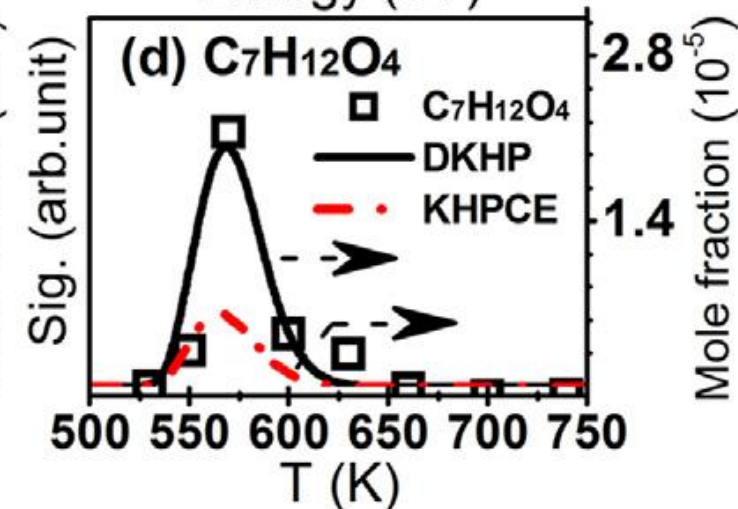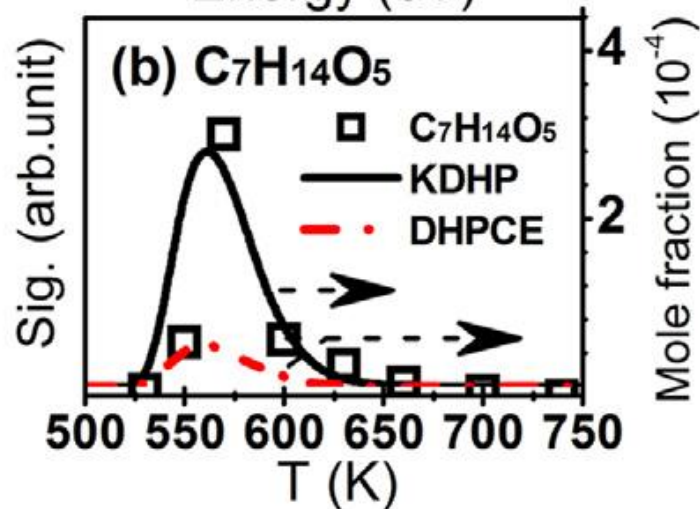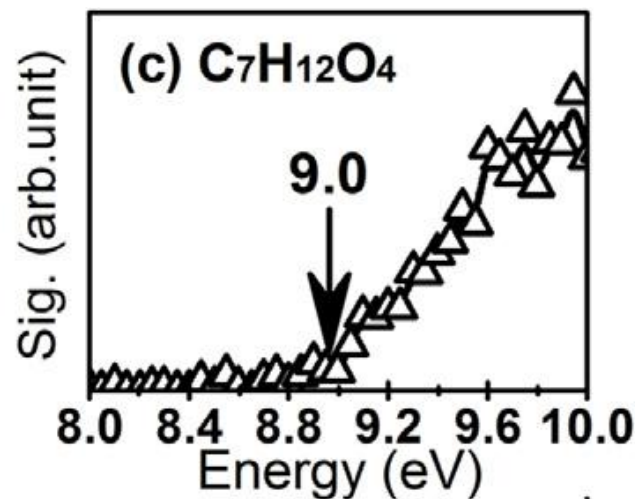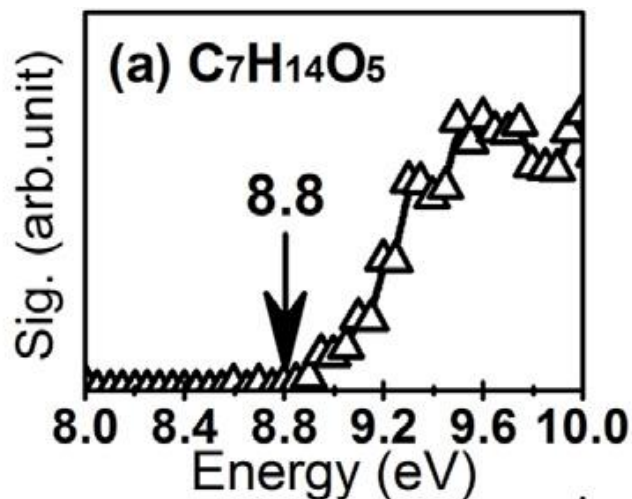
Keto-dihydroperoxide
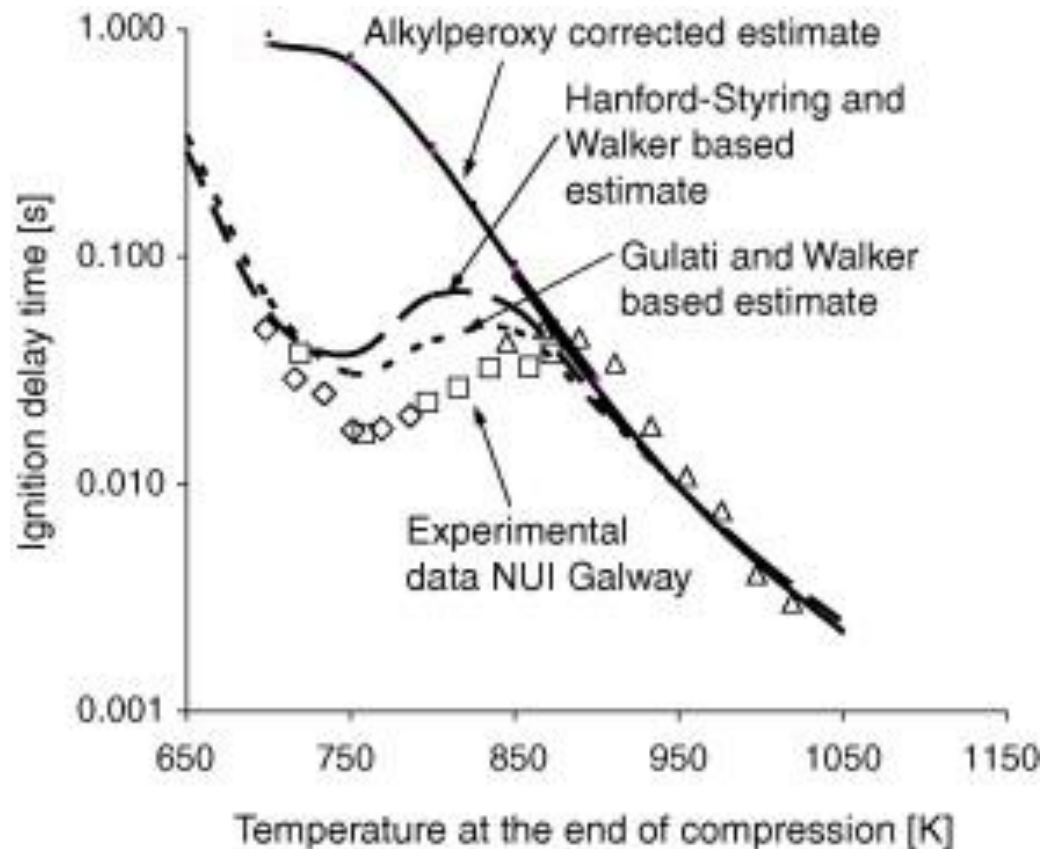Dihydroperoxy cyclic ether

Diketo-hydroperoxide
Ketohydroperoxide cycli ether

Mechanism extensions following obeservations

- Blue arrows show extensions to mechanism of Mohamed et al, J Phys Chem, 120 (2010) 3169

Rapid compression machines and ignition delay times: methyl cyclohexane (Proc Comb Inst, 31, 267 (2007)

- Measured ignition delay times (symbols) for MCH/O_2/diluent stoichiometric mixtures for 10 atm pressure at the end of compression ($\diamond$, 100% N_2; $\square$, 50% N_2/50% Ar; and $\triangle$, 100% Ar). The predicted ignition delays (curves) are for the three estimates of RO_2 isomerization rates for MCH.
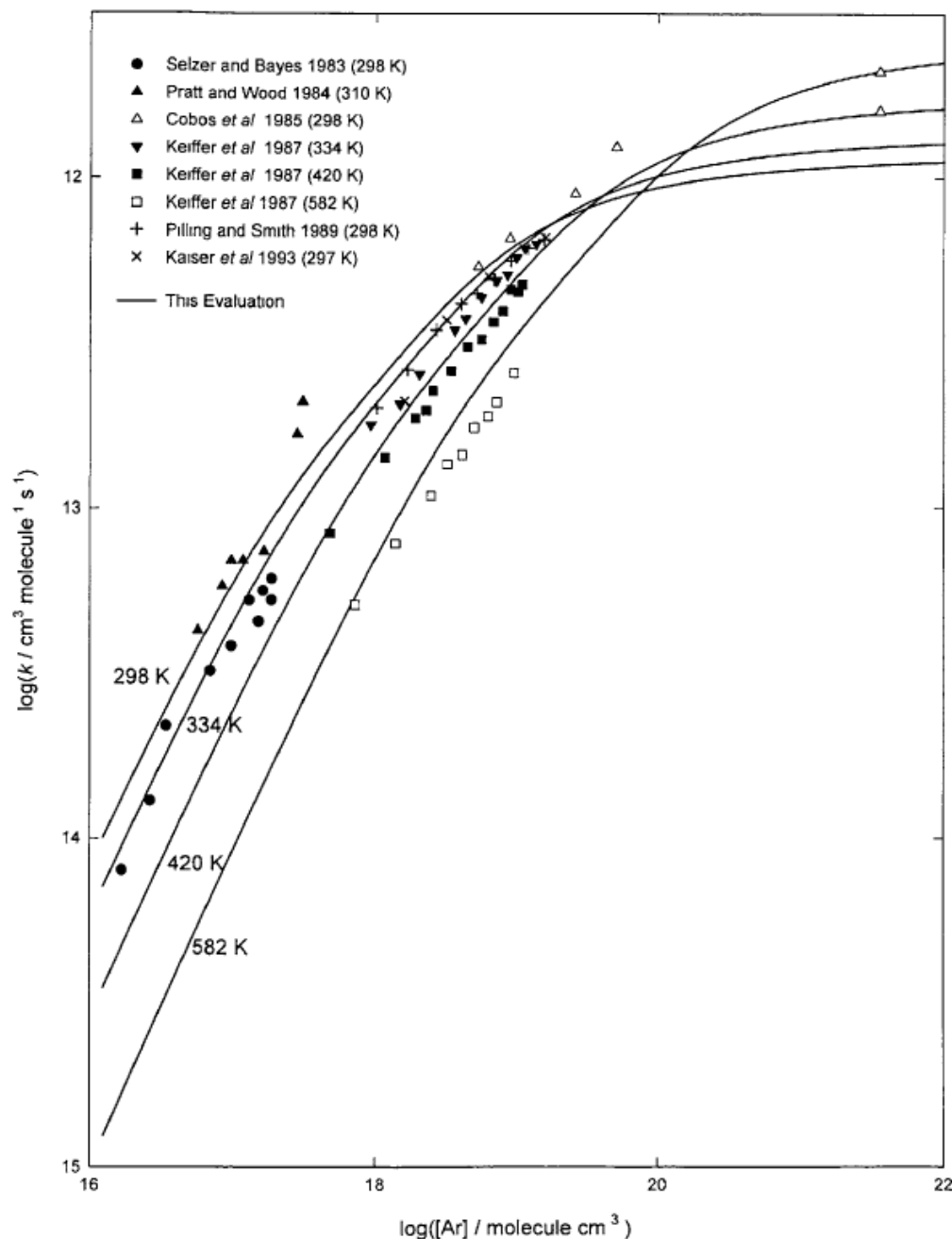
Individual reactions or groups of reactions

CH$_3$ + O$_2$

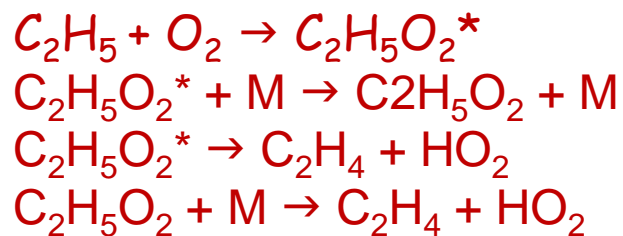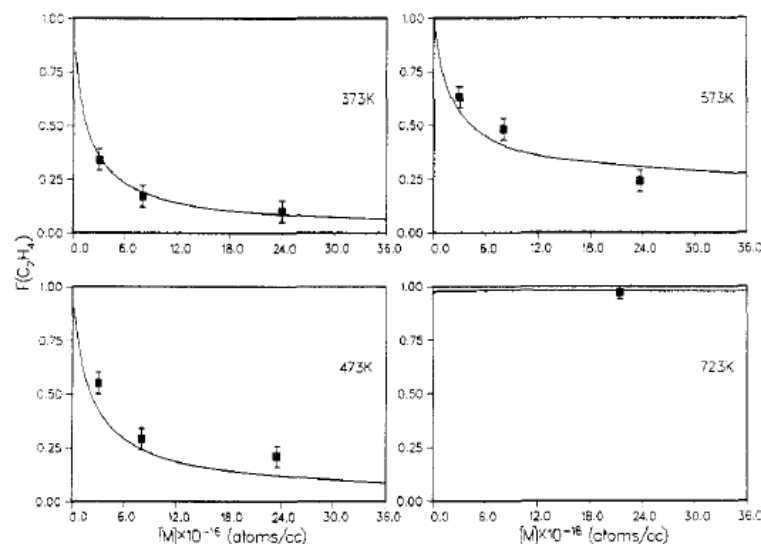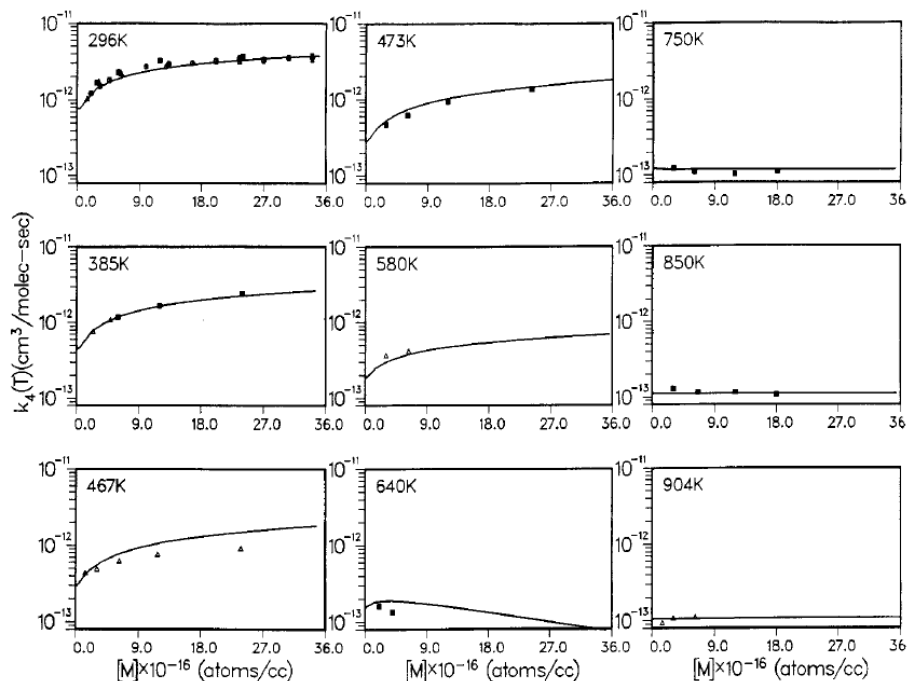Evaluation: J Phys Chem Ref Data, 2005, 34, 757

Shows experimental data with fits using Troe method

Experimental methods: pulsed photolysis and discharge flow

# $C_2H_5 + O_2$; Wagner et al J Phys Chem 94 (1990) 1853
Theory + pulsed photolysis, photionization mass spectrometry

$C_2H_5 + O_2 \rightarrow C_2H_5O_2^*$

$C_2H_5O_2^* + M \rightarrow C2H_5O_2 + M$

$C_2H_5O_2^* \rightarrow C_2H_4 + HO_2$

$C_2H_5O_2 + M \rightarrow C_2H_4 + HO_2$

- The overall rate constant is pressure dependent at low T and beomes pressure independent at high T
- The ethene yield decreases with pressure at low T. It increases with T, and dominates at high T

Electronic structure calculations for $C_2H_5 + O_2$

From Zador Progress in Energy and Combustion Science 37 (2011) 371
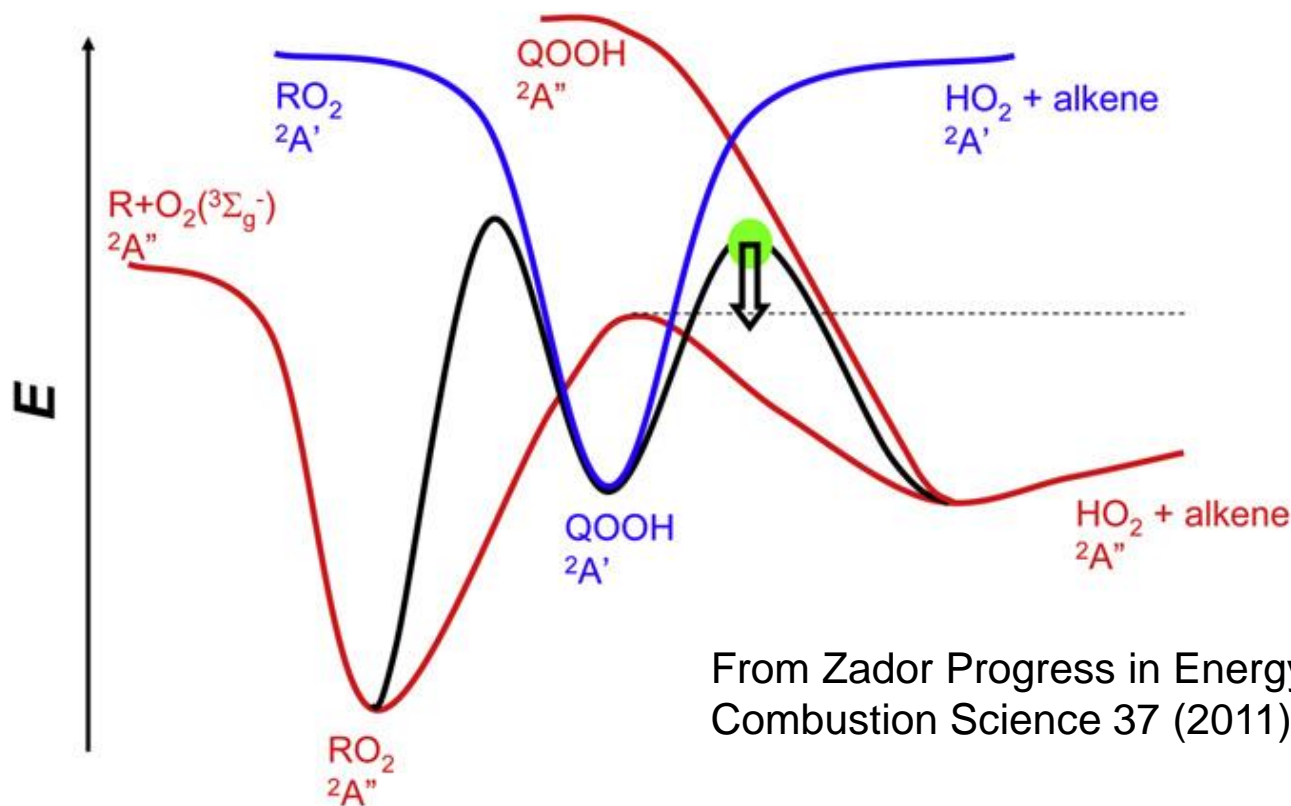
- Two hydrogen-transfer transition states
  - $^2A''$ electronic state
  - ^2A electronic state derived from a 2A' planar structure
- At the best level of theory used, DZP(double zeta plus polarization) CCSD(T) $^2A''$ transition state lies 4.5 kcal mol-' above the reactants
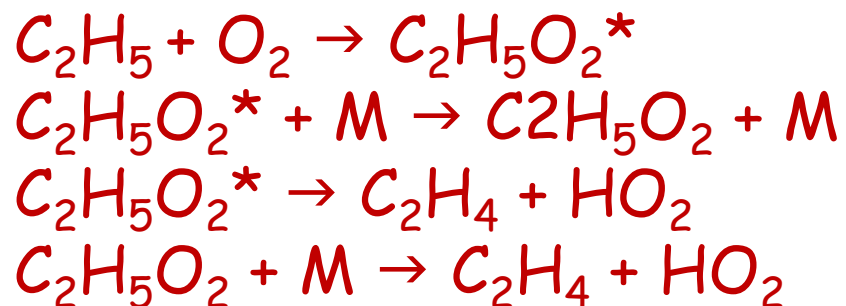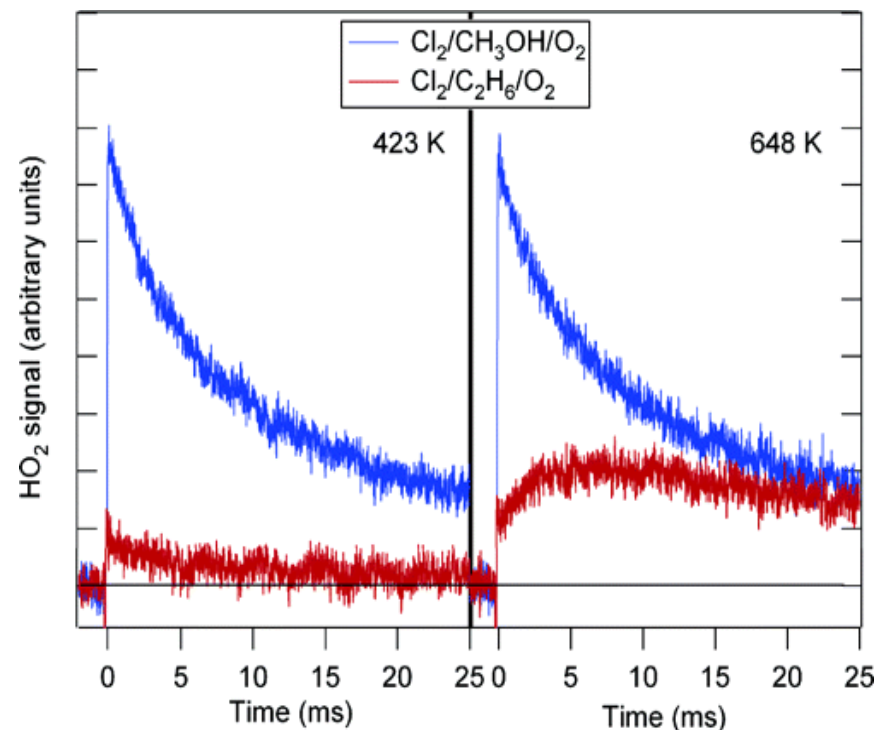
Importance of level of theory in determining the $C_2H_5 + O_2$ PES
(Klippenstein, Proc Comb Inst 36 (2017) 77–111
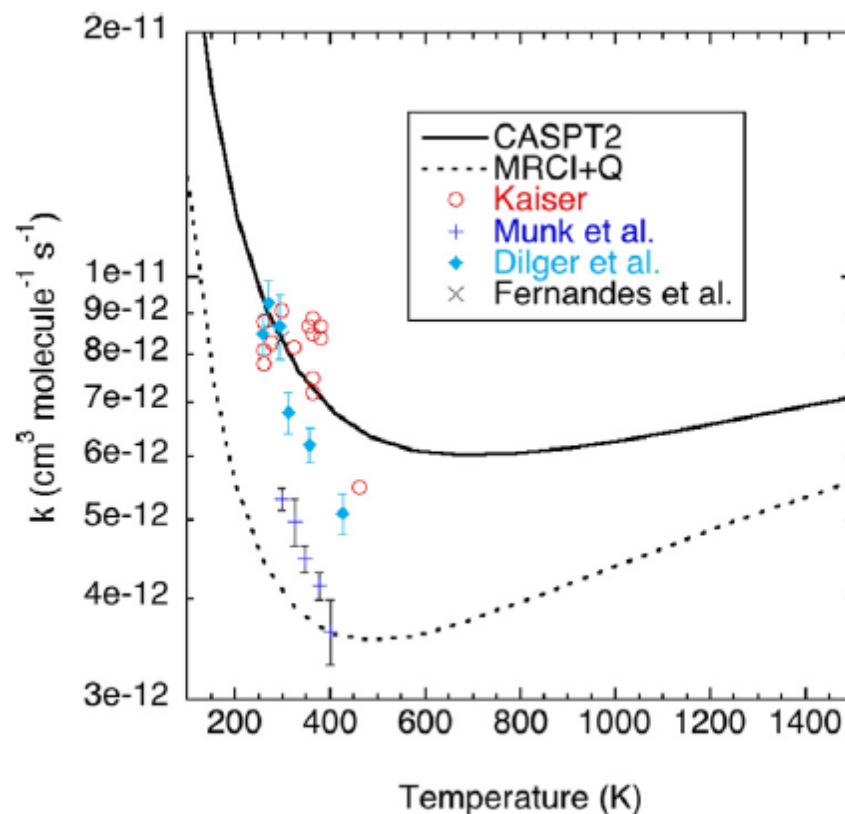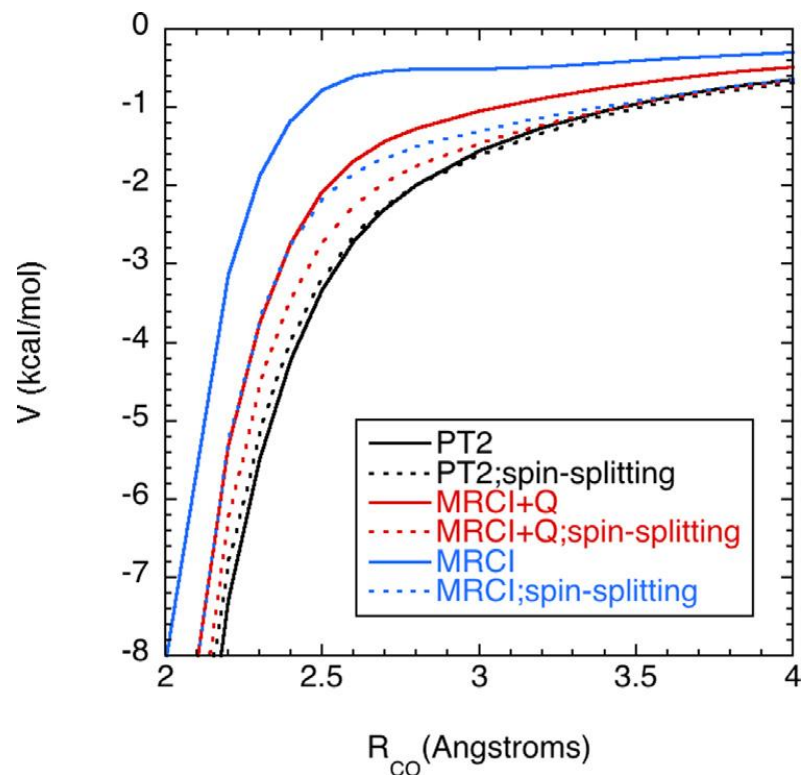
- Plot of the $C_2H_5 + O_2$ interaction energy along the R (C-O) distinguished coordinate minimum energy path. The black, red, and blue lines correspond to CASPT2, MRCI + Q, and MRCI calculations, respectively. The solid lines denote direct calculations of the interaction energy, while dashed lines denote calculations of the doublet–quartet splitting combined with CCSD(T) calculations of the quartet interaction energy.
- Rate constant: theory, high pressure limit; experiment: 1 atm except Fernandes, 100 atm

Determination of product yields in $C_2H_5 + O_2$ pulsed photolysis at higher pressures
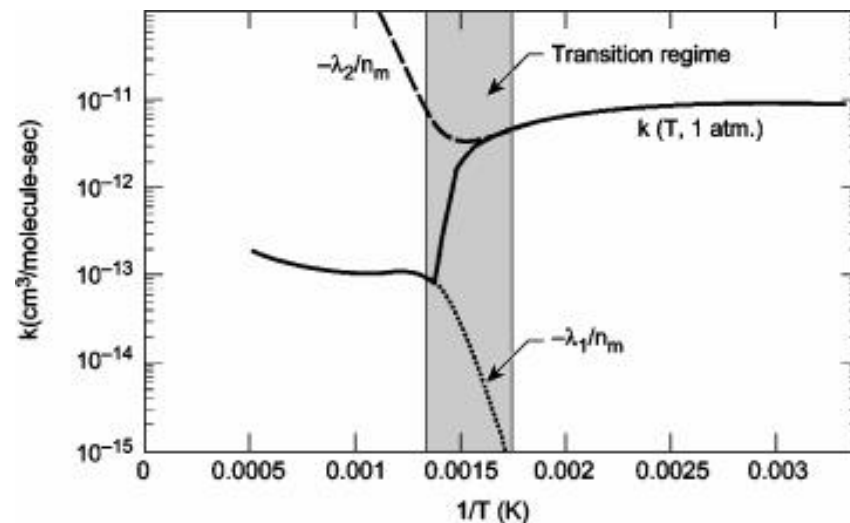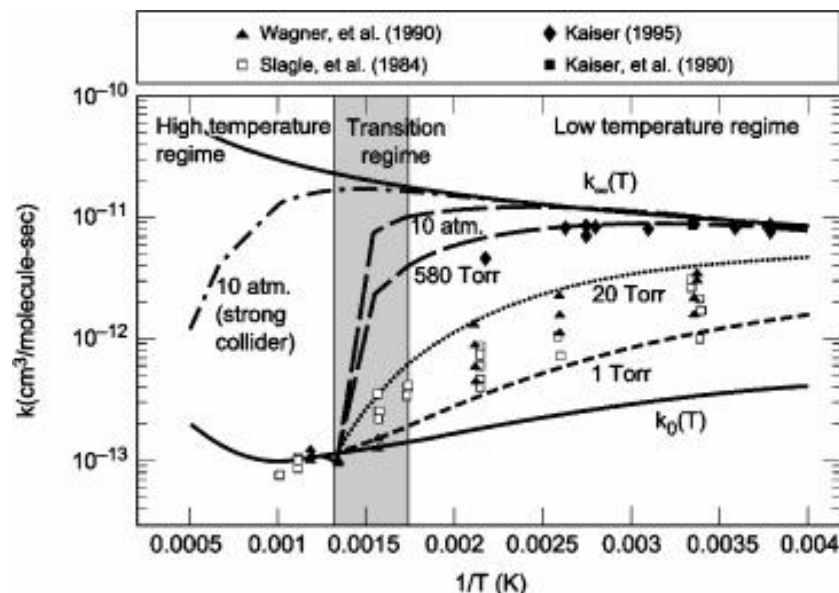
- Taatjes et al. (J. Phys. Chem. A 104 (2000) 11549 – 11560) observed the formation of OH and HO_2, determining the fractional yields. Used 100% yield of HO_2 from $CH_2OH + O_2$ to calibrate the system.

- HO_2 yield↑ as T↑ and p↓

- Two timescales at higher T

- OH yield is small.

$$C_2H_5 + O_2 \rightarrow C_2H_5O_2*$$
$$C_2H_5O_2* + M \rightarrow C2H_5O_2 + M$$
$$C_2H_5O_2* \rightarrow C_2H_4 + HO_2$$
$$C_2H_5O_2 + M \rightarrow C_2H_4 + HO_2$$

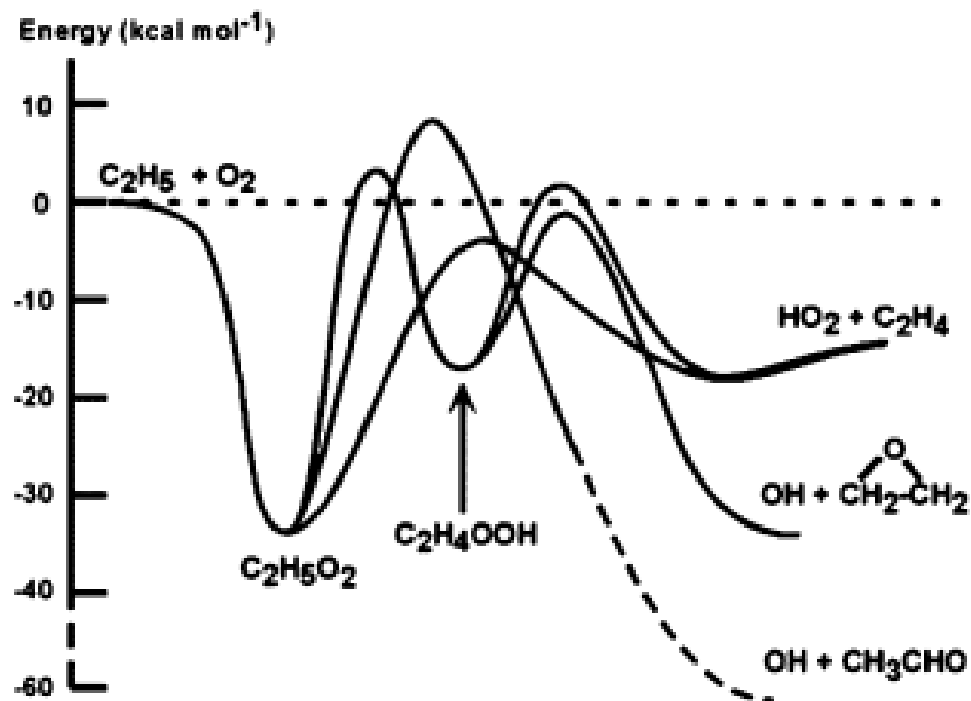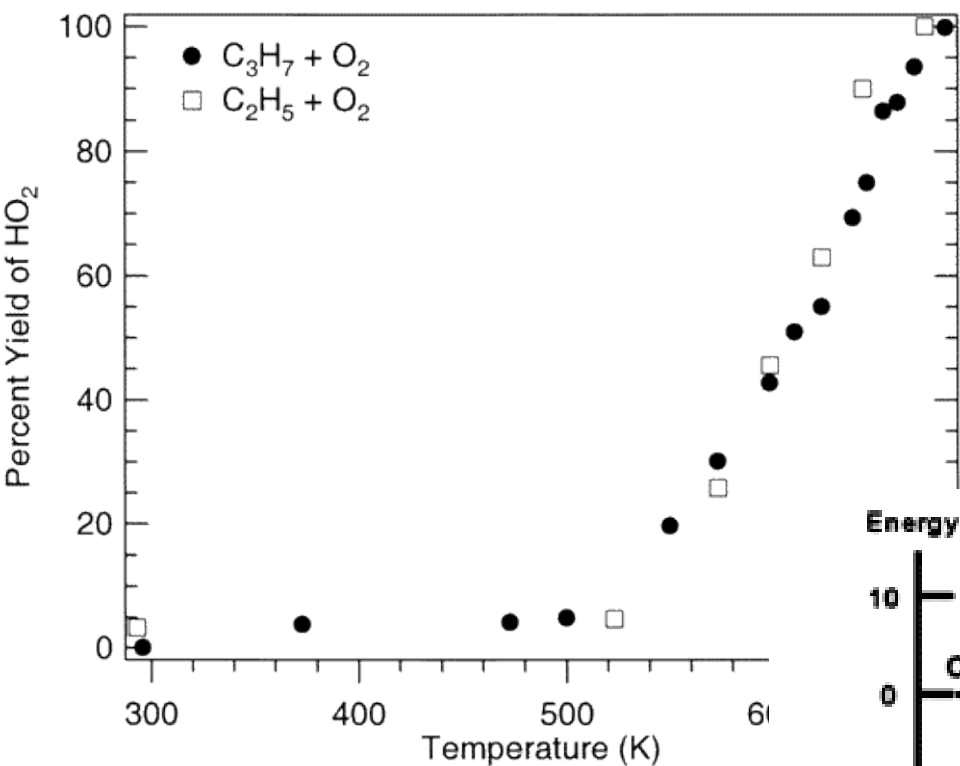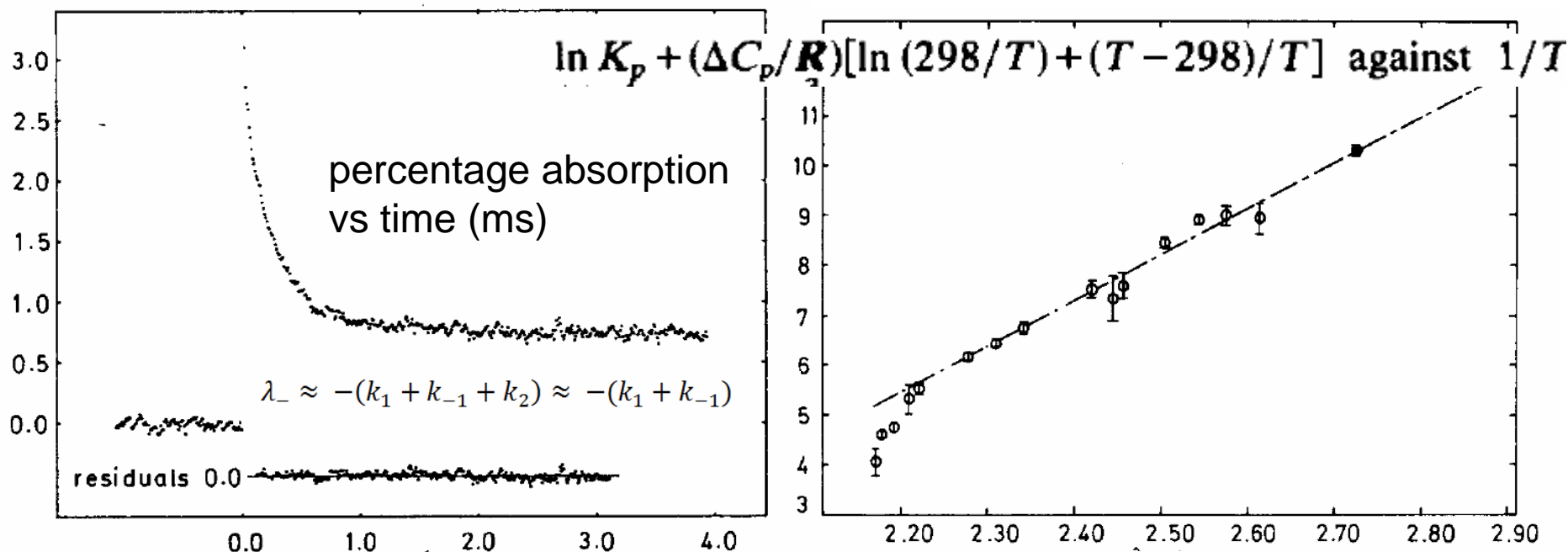# Master equation analysis: Miller and Klippenstein,

- Three regimes, low, transition, high T.
- In transition region, thermal rate constant jumps from one eigenvalue to the other – the two eigenvalues are mixed in this region.
- At high T, ethyl peroxy is stabilised and HO_2 is formed from its dissociation. k is, in practical terms, independent of p.
- At low T, reaction involves the pressure dependent formation of RO_2 and direct formation of HO_2

$C_2H_5, C_3H_7 + O_2$

$R + O_2 \rightleftharpoons RO_2$ (R = allyl)

Morgan et al JCS Faraday Trans 2 78, 1323-1330 (1982)

percentage absorption vs time (ms)

$$\lambda_- \approx -(k_1 + k_{-1} + k_2) \approx -(k_1 + k_{-1})$$

residuals 0.0

$\ln K_p + (\Delta C_p / R)[\ln (298/T) + (T - 298)/T]$ against $1/T$

R	$-\Delta H^{\ominus}_{298}$ [a]	$-\Delta S^{\ominus}_{298}$ [a]	T_c/K
CH_3	127	126	862
C_2H_5	121	135	778
$i\text{-}C_3H_7$	129	144	776
$t\text{-}C_4H_9$	131	166	709
C_3H_5	75	122	547
	(76.2 ± 2.1)	(122 ± 5)	(550 ± 5)[b]
$C_6H_5CH_2$	70	122	503

- Estimated enthalpies and entropies of reaction in kJ mol^{-1}
- (b) experimental values
- Ceiling temperatures/ K (0.1 atm O_2)

# Radical dissociation: 1-butyl
Knyazev and Slagle, J. Phys. Chem. 1996, 100, 5318-5328
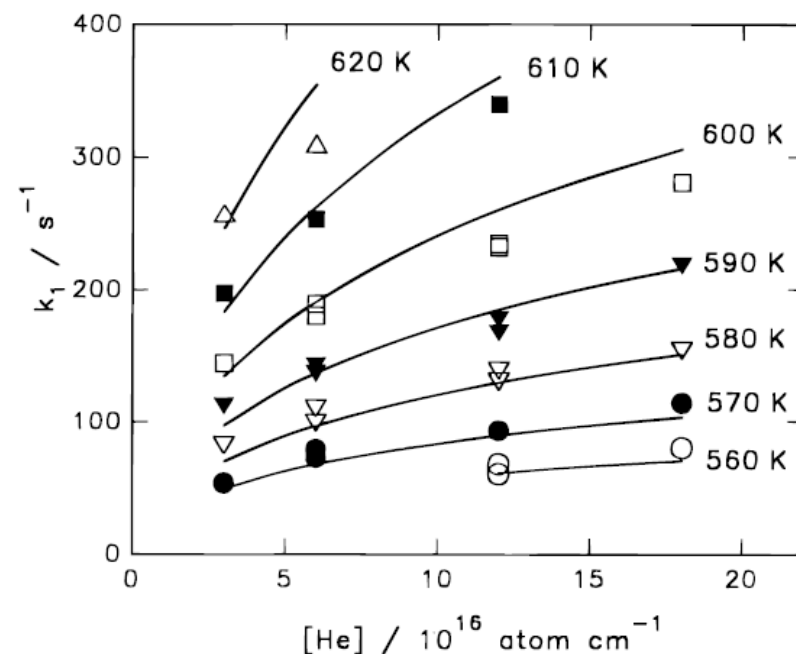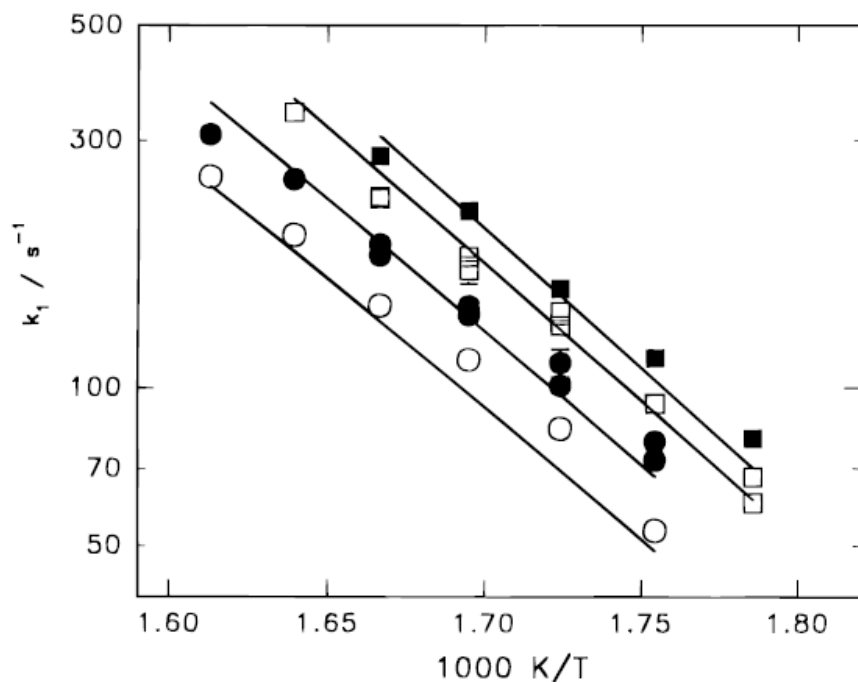
- Pulsed photolysis, photoionization mass spectrometry
- Data fitted with master equation analysis, coupled with TS model based on electronic structure calculations
- Gave limiting high and low pressure rate constants and fall off data based on Troe modification of Lindemann Hinshelwood model

A detailed example: $CH_3OCH_2 + O_2$
1. OH + dimethyl ether (Carr et al. J. Phys. Chem. A 2013, 117, 11142–11154
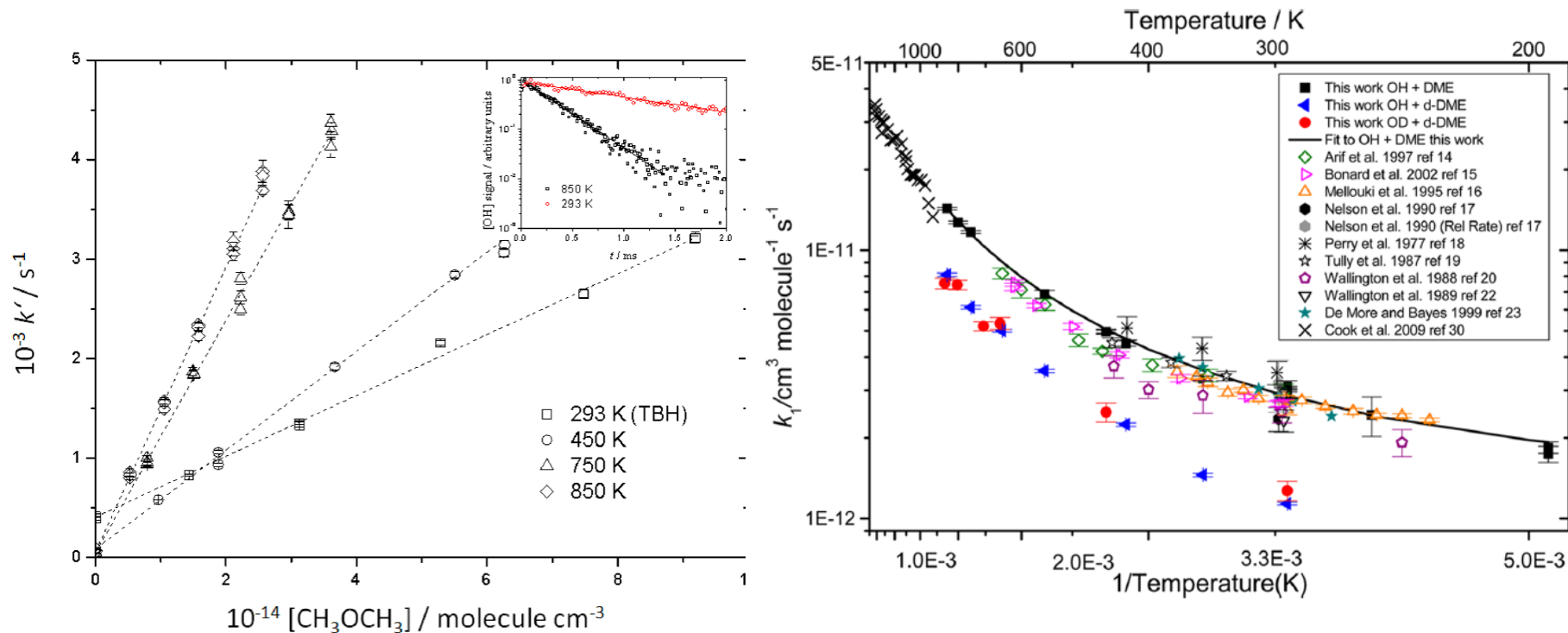
- Left hand plot shows examples of experimental decays using pulsed photolysis / laser induced fluorescence. Main figure shows examples of bimolecular plots (first order decay constant from individual experiments vs $[CH_3OCH_3]$. Experiments over the range 195 – 850 K

- Right hand plot shows these data and literature data, with fit giving
  k = (1.54±0.48)×(T/298 K)1.89±0.16exp(-184±112) cm3 molecule-1 s-1 (195 – 1423 K)
  Errors are 95% confidence limits)

- Note the results from isotope substitution: blue – OH + d-DME, red OD + d-DME – used in fits to theory

$$k(T) = \alpha \frac{kT}{h} \frac{Q_{TS}^{\ddagger}}{Q_A Q_{BC}} \exp\left(\frac{-\Delta\varepsilon_0}{kT}\right)$$

Fits to theory
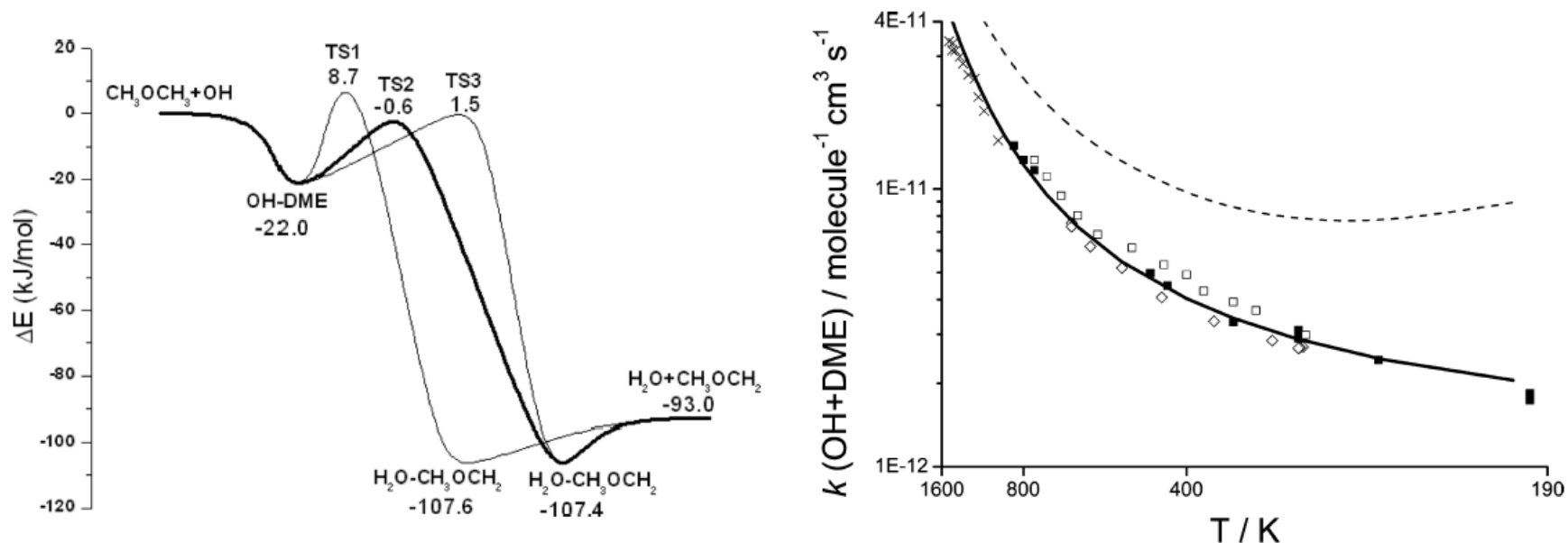
- Left hand plot shows turning points on PES: Geometric parameters were optimized at the CCSD/AVDZ level and the energies were calculated at the FCC/CBS//CCSD/AVDZ level with zero-point energy corrections.

- Right hand plot shows best fit. Dashed line with no adjustments to theory. Full line – best fit barrier energy adjusted to +0.6 kJ mol-1, hindrance parameters scaled by factor of 2.5. Tunnelling using WKB method, reaction path calculated at CCSD(T)/aug-cc-pVDZ level of theory.

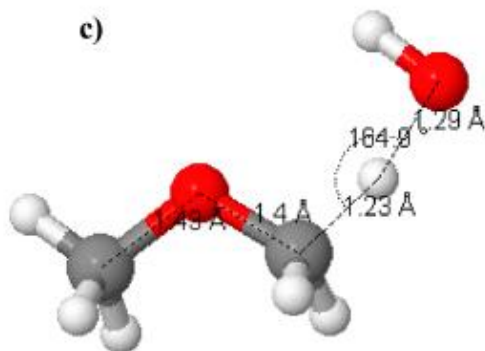- Used two transition state model, using a master equation analysis
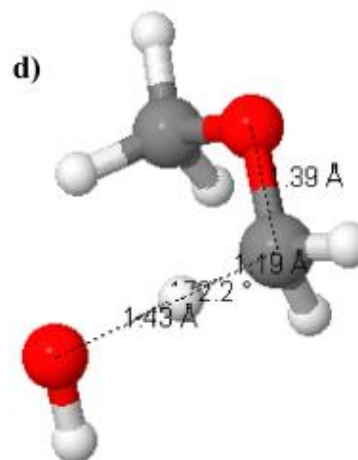
3 transition states – not all independent

a)

0.99 Å
177.1 °
1.86 Å
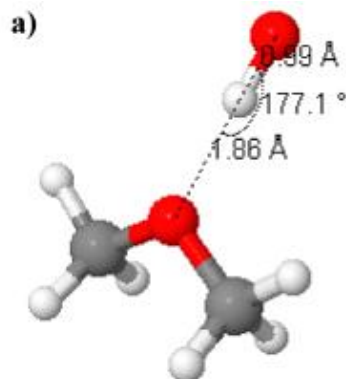
Initial OH/DME complex with C_{2v}
or C_s symmetry

b)

1.42 Å
1.4 Å
173.2 °
1.19 Å
1.42 Å
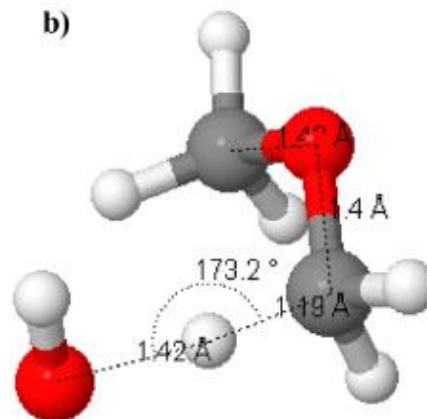
TS2 Out-of-plane transition state
with upward pointing OH

c)

1.29 Å
164.9
1.43 Å 1.4 Å 1.23 Å

TS1 - In-plane transition state with
C_s symmetry

d)

1.39 Å
1.19 Å
172.2 °
1.43 Å

TS3 Out-of-plane transition state
with downward pointing OH
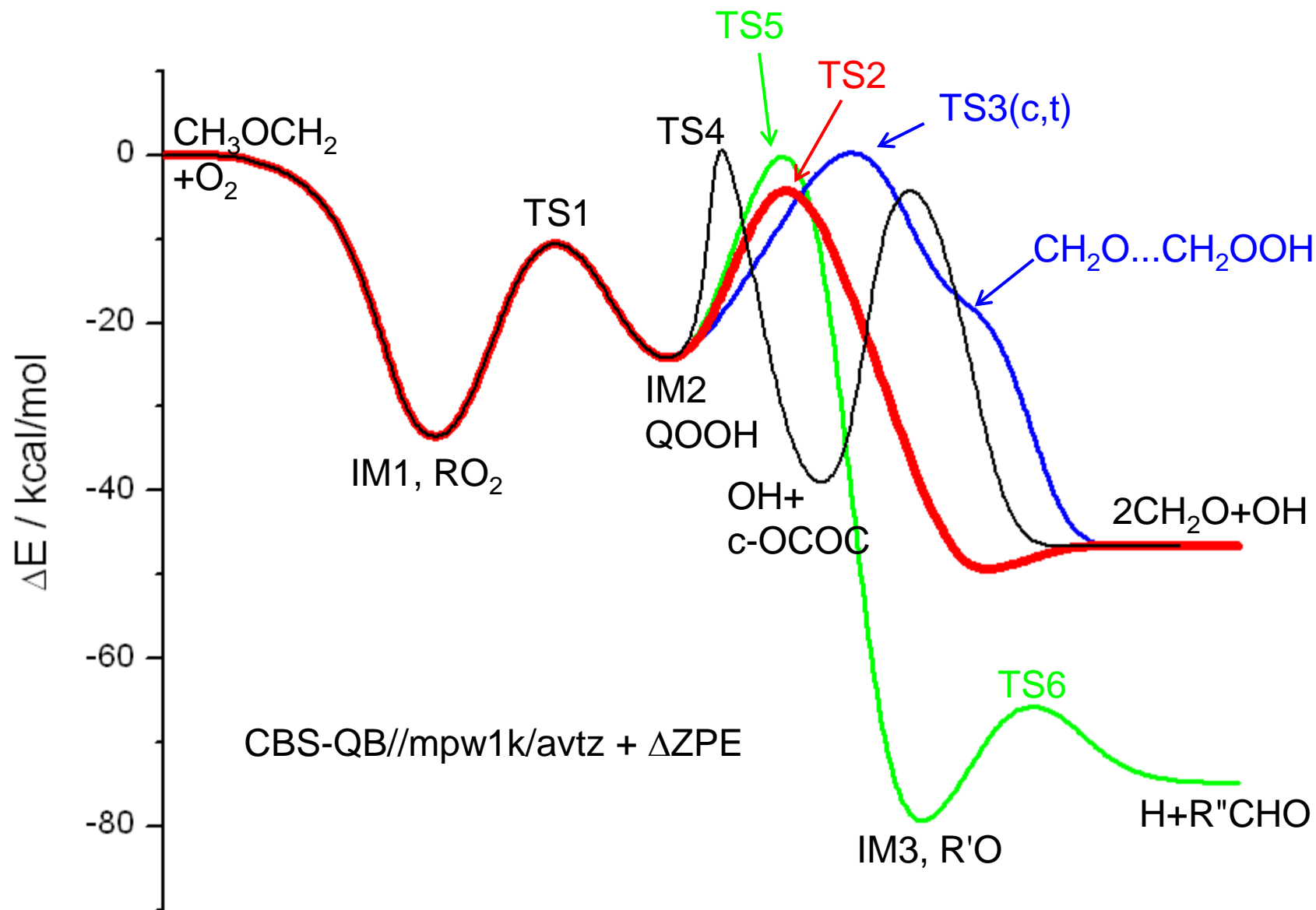
$CH_3OCH_2 + O_2$
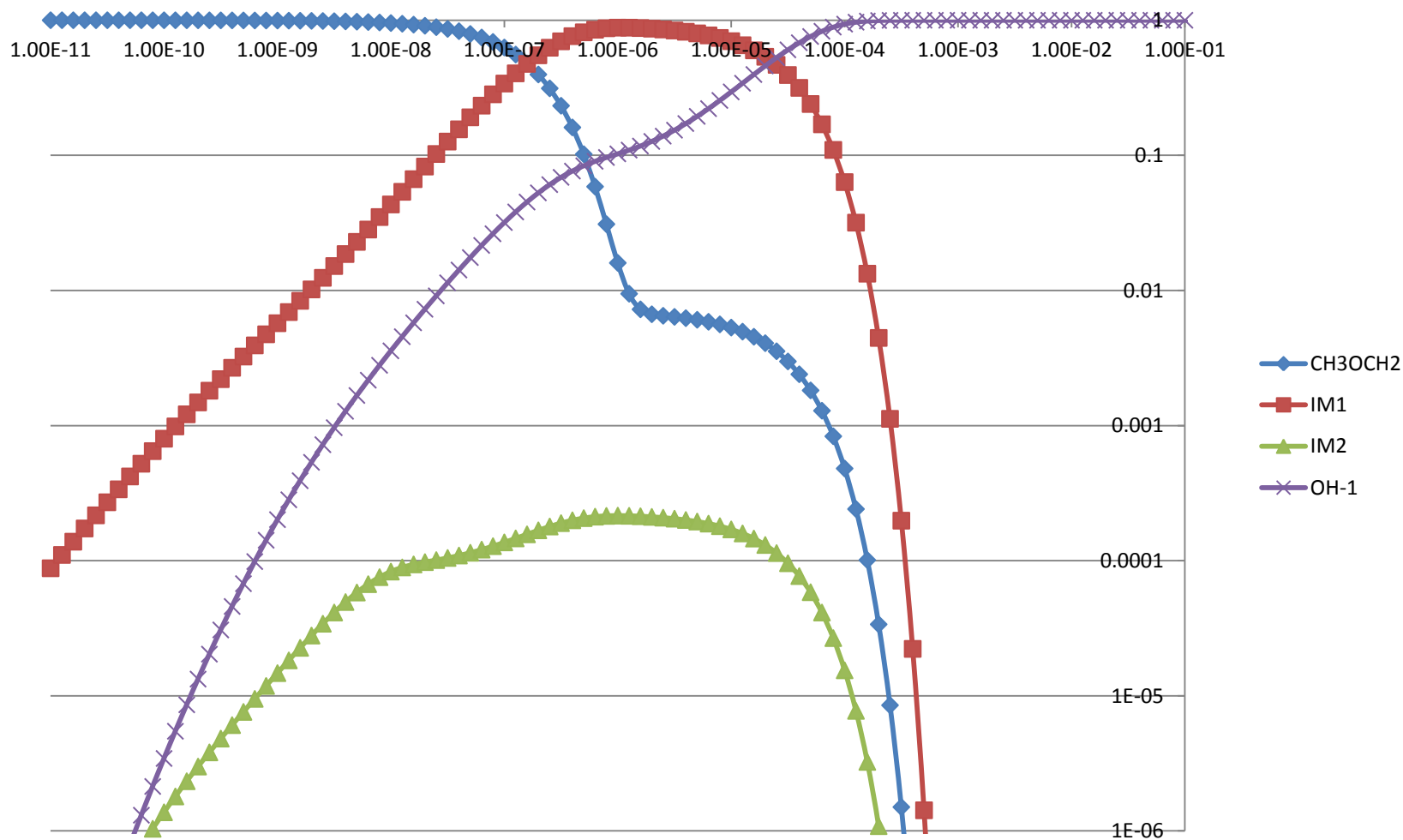## Eskola et al. J. Phys. Chem. A 2014, 118, 6773–6788

Pulsed laser photolysis, laser induced fluorescence detection of OH
Measured the yield of OH and the rate constants via the formation of OH
Fits to data varying association rate constant (A,n), energy transfer
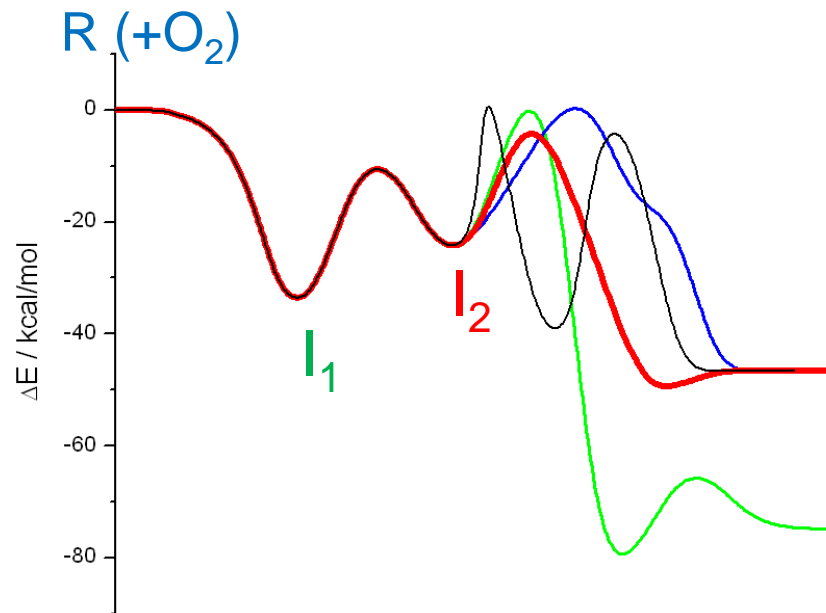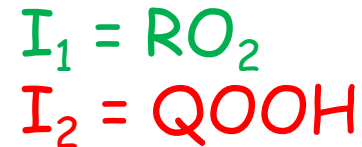parameters and some TS parameters
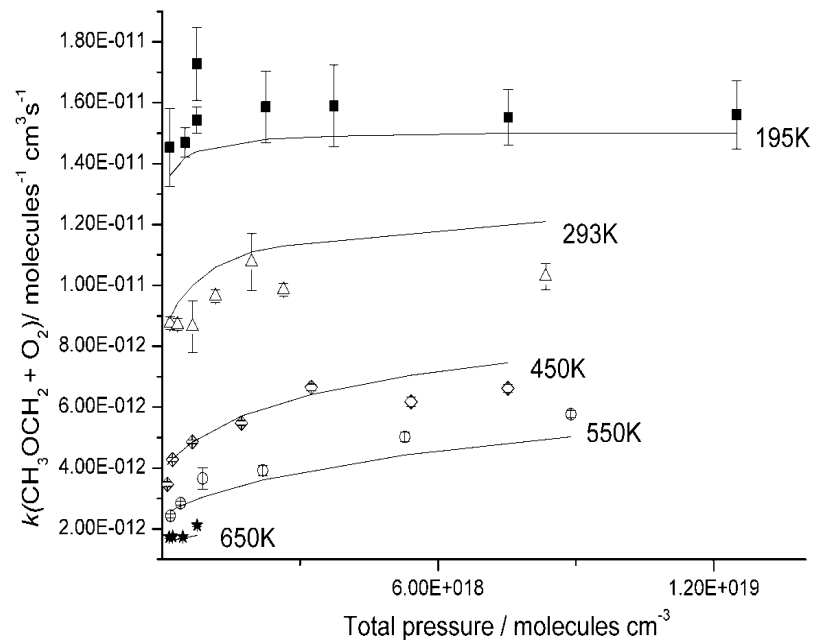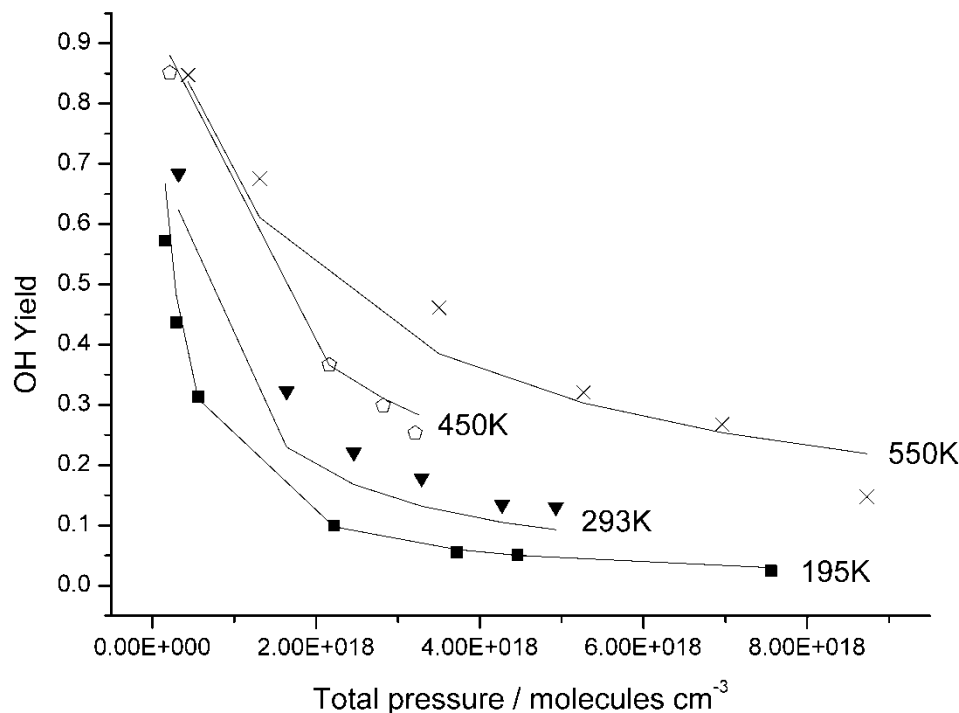
CH$_3$OCH$_2$ + O$_2$: major mechanism

TS5

TS2

TS3(c,t)

CH$_3$OCH$_2$
+O$_2$

0

TS4

TS1

CH$_2$O...CH$_2$OOH

ΔE / kcal/mol

-20

IM2
QOOH

IM1, RO$_2$

OH+
c-OCOC

2CH$_2$O+OH

-40

CBS-QB//mpw1k/avtz + ΔZPE

-60

TS6

-80

IM3, R'O

H+R"CHO
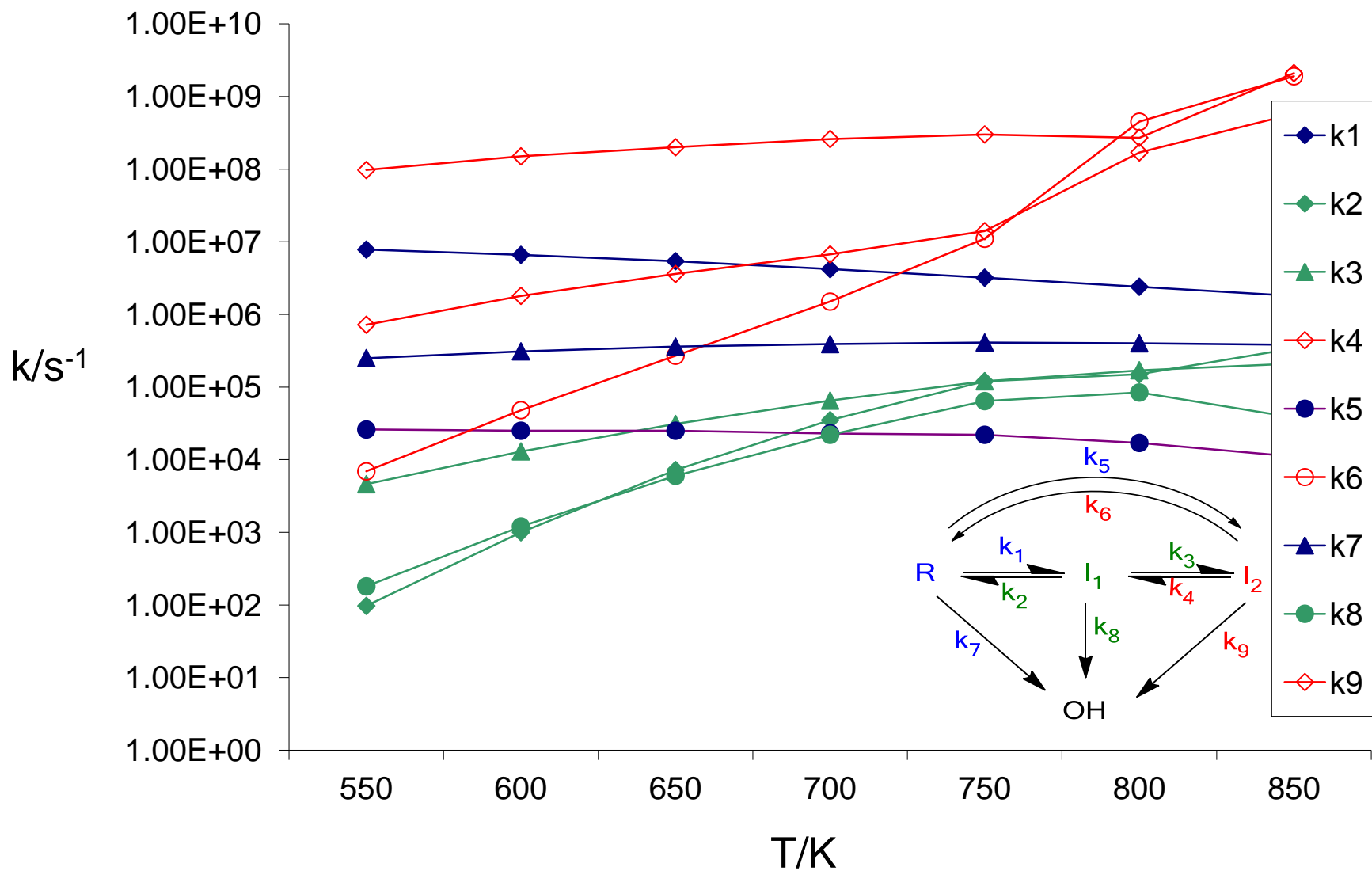
Master equation analysis. Species profiles, 550 K, 1 bar

Master equation: rate constant analysis
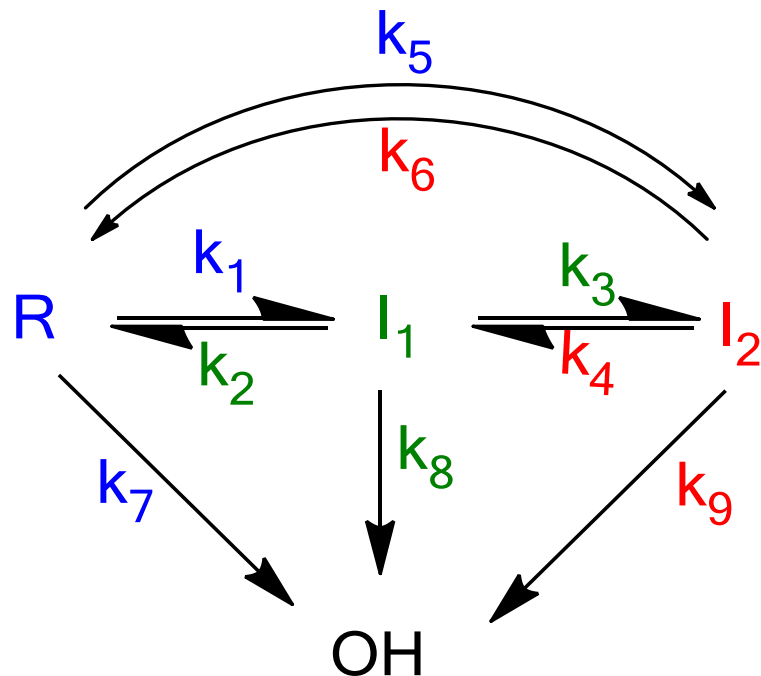
Phenomenological rate ceoefficients from a Bartis Widom analysis

Analytic expressions for the two smallest eigenvalues

- Lifetime of IM2 (=QOOH) is always much less than those for R and RO2
- Let x=R, y=RO2, z = QOOH. Apply QSSA z

$$z = \frac{k_5 x + k_3 y}{k_4 + k_6 + k_9}$$

$$\frac{d\mathbf{c}}{dt} = \begin{pmatrix} -(k_1 + k_5(1 - \frac{k_6}{k}) + k_7) & k_1 + \frac{k_5 k_4}{k} \\ k_2 + \frac{k_3 k_6}{k} & -(k_2 + k_3(1 - \frac{k_4}{k}) + k_8) \end{pmatrix} \mathbf{c} = \begin{pmatrix} -A & B \\ C & -D \end{pmatrix} \mathbf{c}$$
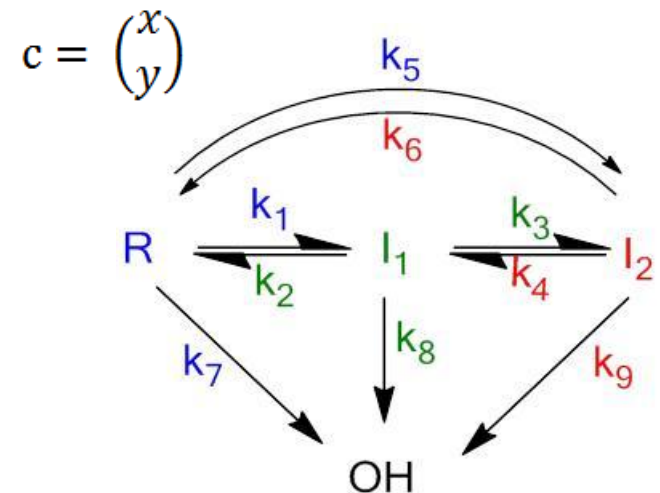
$$\lambda_{\pm} = \frac{-(A + D) \pm \sqrt{(A + D)^2 - 4(AD - BC)}}{2}$$

$$\mathbf{c} = \begin{pmatrix} x \\ y \end{pmatrix}$$
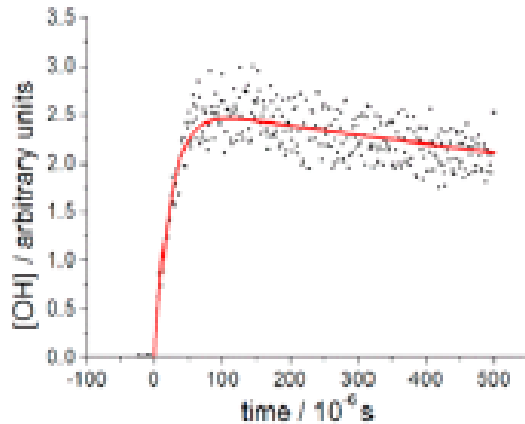
If $(A + D)^2 \gg 4(AD\text{-}BC)$, binomial expansion gives

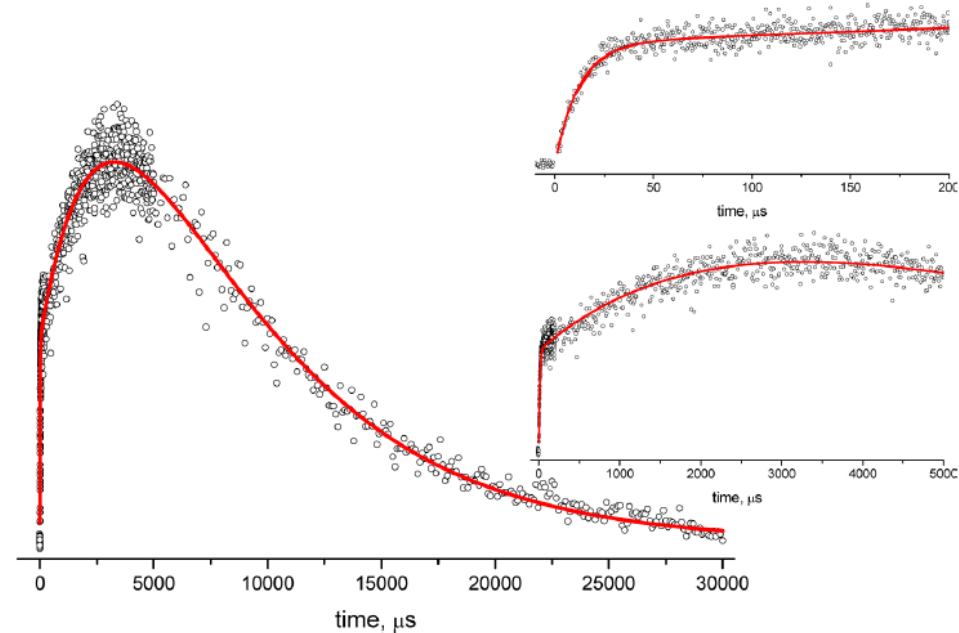$$\lambda_{-} = -(A + D)$$

$$\lambda_{+} = \frac{-(AD - BC)}{A + D}$$

- CSEs from master equation solution. Two smallest eigenvalues are λ_1, λ_2
- $\lambda_1 = \lambda_{+}$; $\lambda_2 = \lambda_{-}$

# Time dependence of the OH profiles at 300 K and at 550 K

- At low T, the OH signal is biexponential.
- The decay corresponds to loss of OH, e.g. by diffusion from the reaction zone and reaction.
- The increase corresponds to λ_2

- At higher T, the signal becomes triexponential.
- The fast rise is λ_2 and the slower rise is λ_1; the decay is again loss of OH

Global Uncertainty Propagation and Sensitivity Analysis in the CH3OCH2 + O2 System: Combining Experiment and Theory To Constrain Key Rate Coefficients in DME Combustion
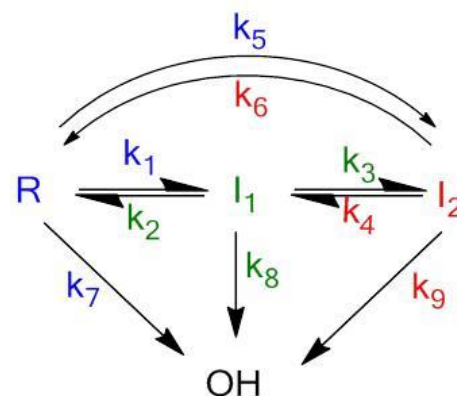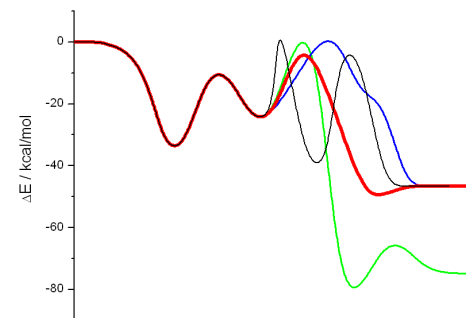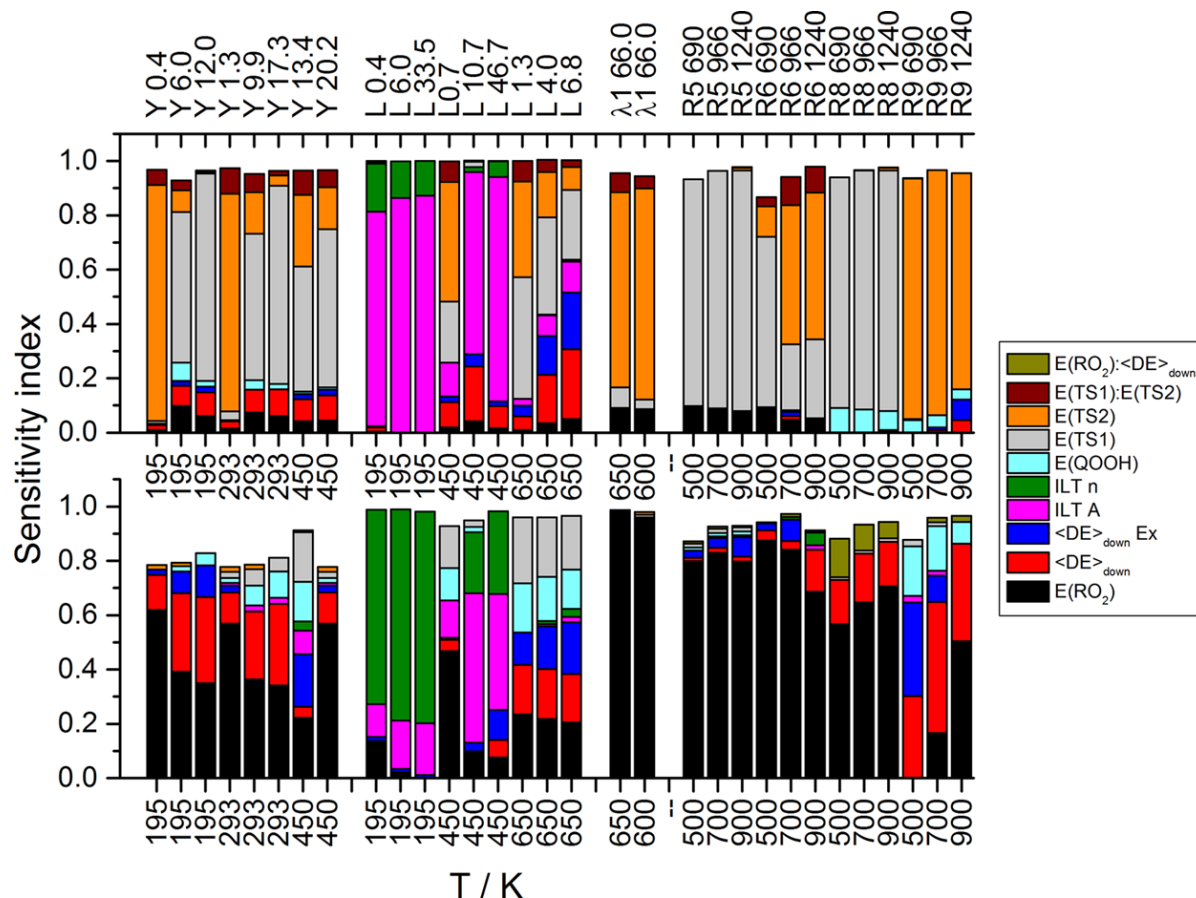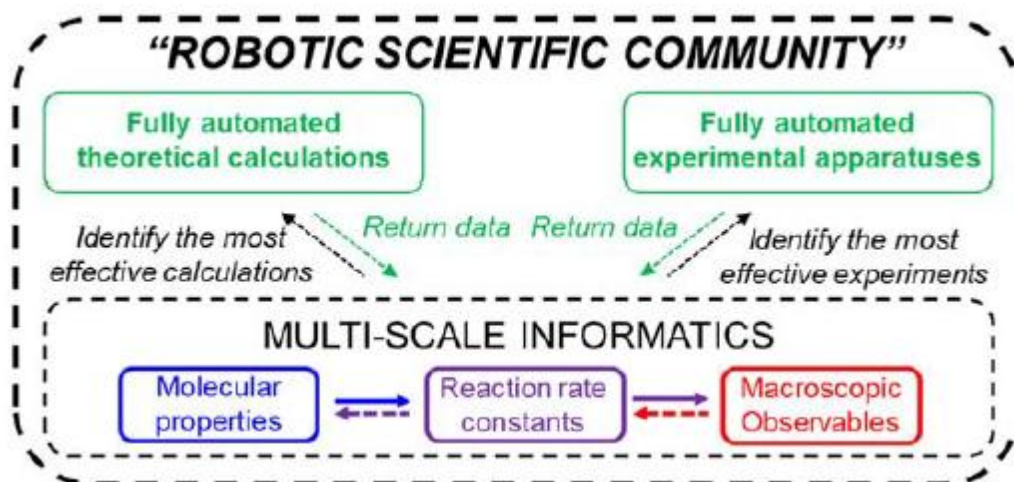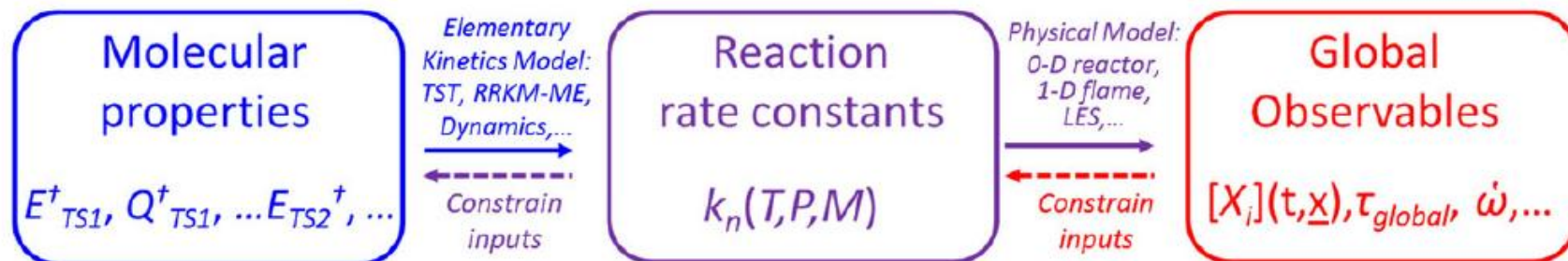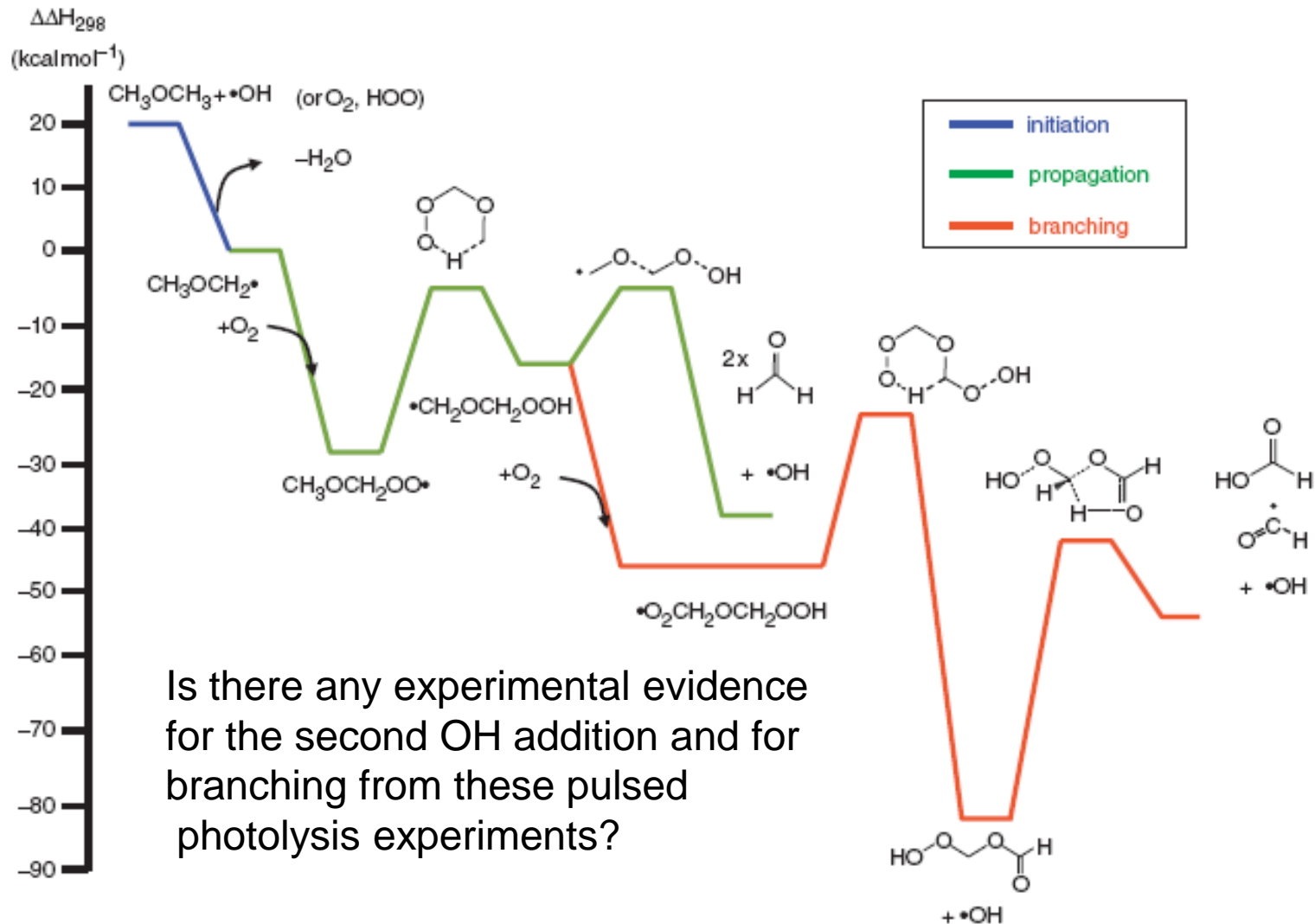
Sensitivity indices for the parameters involved in the master equation modeling with theory-constrained parameter ranges (top) and experimentally constrained parameter ranges (bottom). The labels on the top axis give the pressure at which the calculations were run in kPa and identify the type of observable: Y indicates the OH yield, L indicates the rate coefficient for CH2OCH3 loss, $\lambda 1$, indicates the time constant corresponding to the longer time formation of OH and R indicates a particular elementary rate coefficient. Where the sensitivities sum to be significantly less than 1, this can be attributed to contributions from the second-order sensitivities that are not included. Where there is a colon between two parameters, this indicates a second-order sensitivity for this pair of inputs.

Harnessing the Combined Power of Theoretical and Experimental Data through Multiscale Informatics

Routes to branching: $CH_3OCH_2 + O_2 (+ O_2)$

Is there any experimental evidence for the second OH addition and for branching from these pulsed photolysis experiments?

- Anderson and Carter: Molecular Physics 2008, 106, 367–396

Difficulty of observing second O2 addition with this experimental system
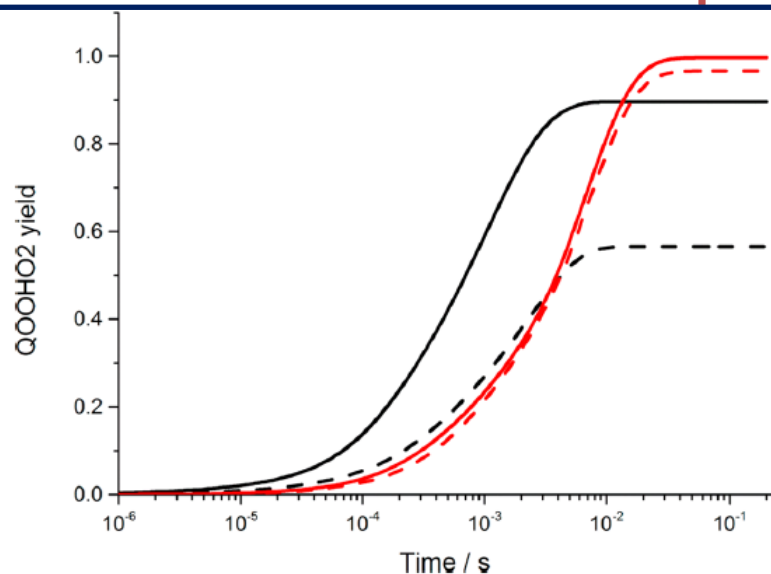
Simulated O_2QOOH formation using a model based upon MESMER rate coefficients from Eskola et al

(black) at 1 bar (solid line) and 10 bar (dashed line) of air (T = 550

K). These are compared with results using rate coefficients from the

Fischer, Dryer, Curran model (red) (Int J Chem Kinet (32, 741, 2000) see slides 7-9).
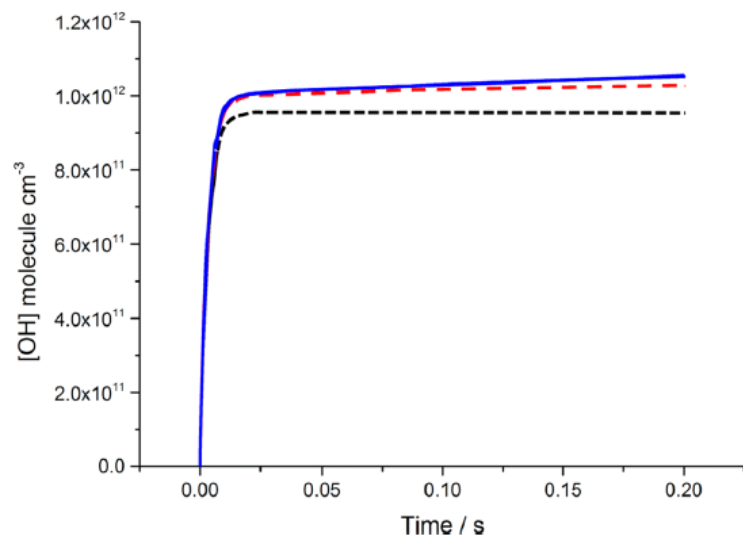
OH simulation at 550 K and 500 Torr with $[O2] = 1 \times 10^{17}$ molecule cm^{-3}: $QOOH + O_2$ rate coefficient of:

 0(black short dashed line),

1.16×10^{-12} cm^3 molecule^{-1} s^{-1} (red long dashed line),

2.32×10^{-12} cm^3 molecule^{-1} s^{-1} (blue solid line)
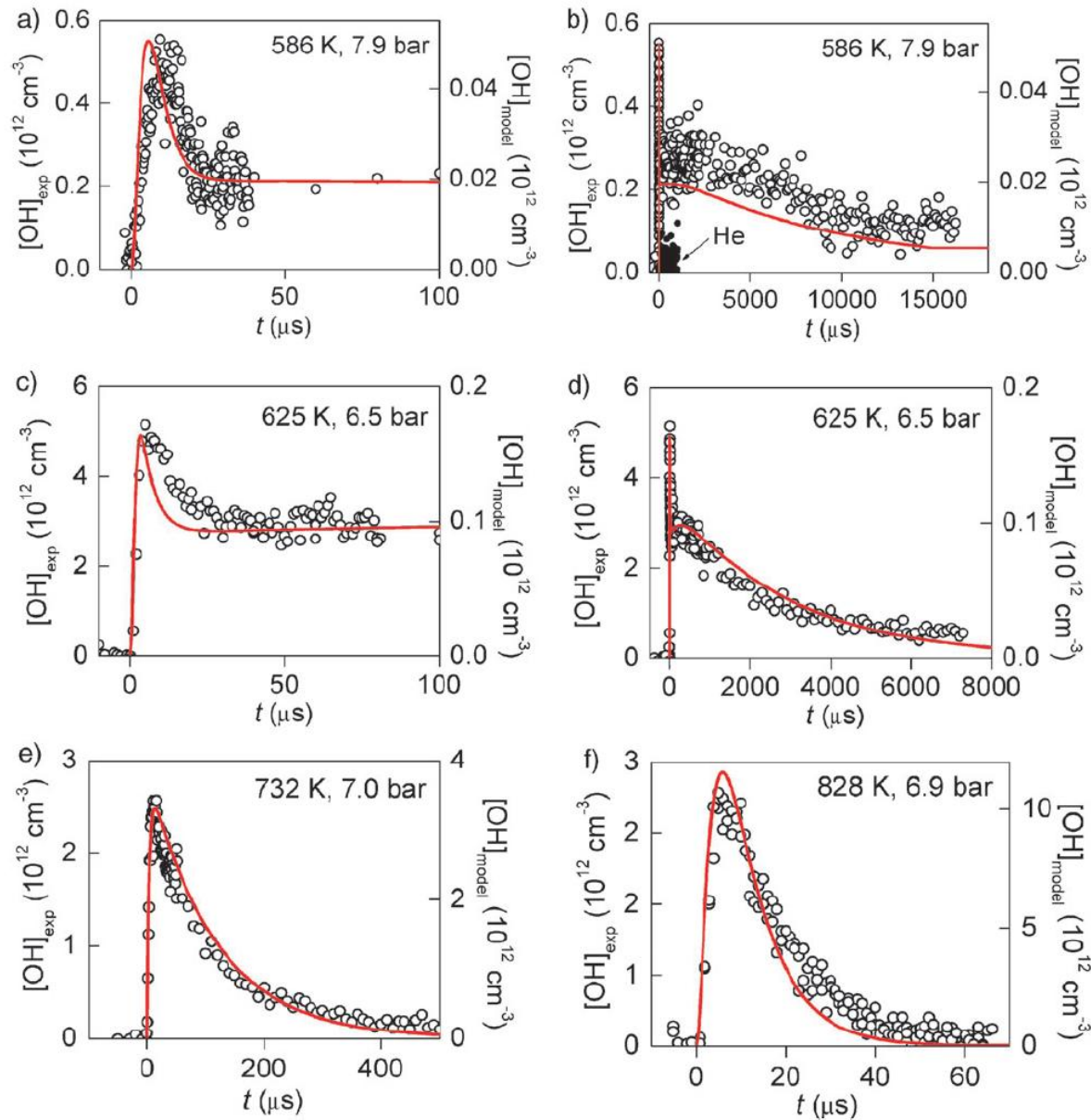
Effect on OH is small and at long times

Cyclohexyl + O2
Fernendes et al. Phys Chem. Chem. Phys., 2009, 11, 1320 -1327
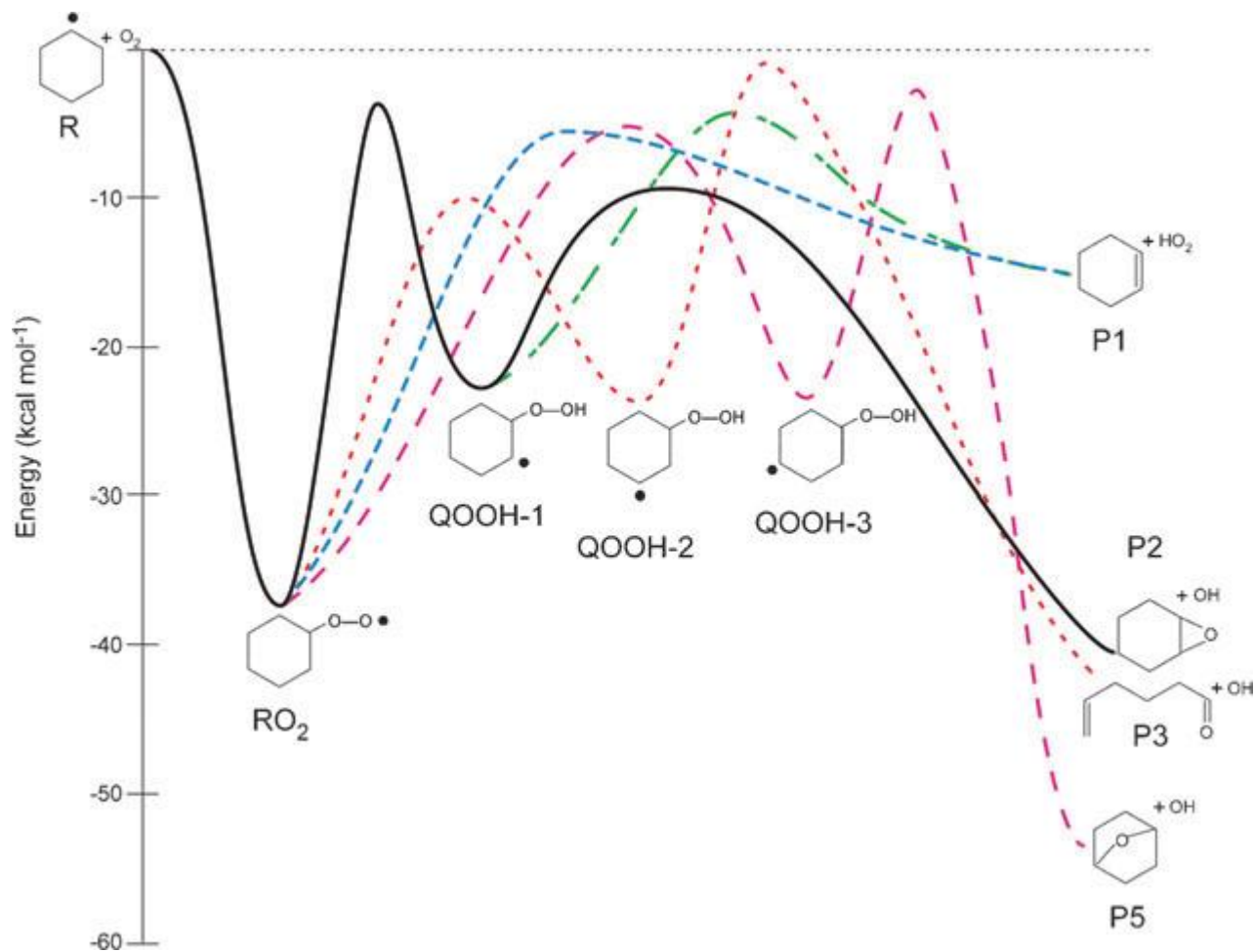
Time dependence of OH formation

Importance of well-skipping (formally direct) route to OH
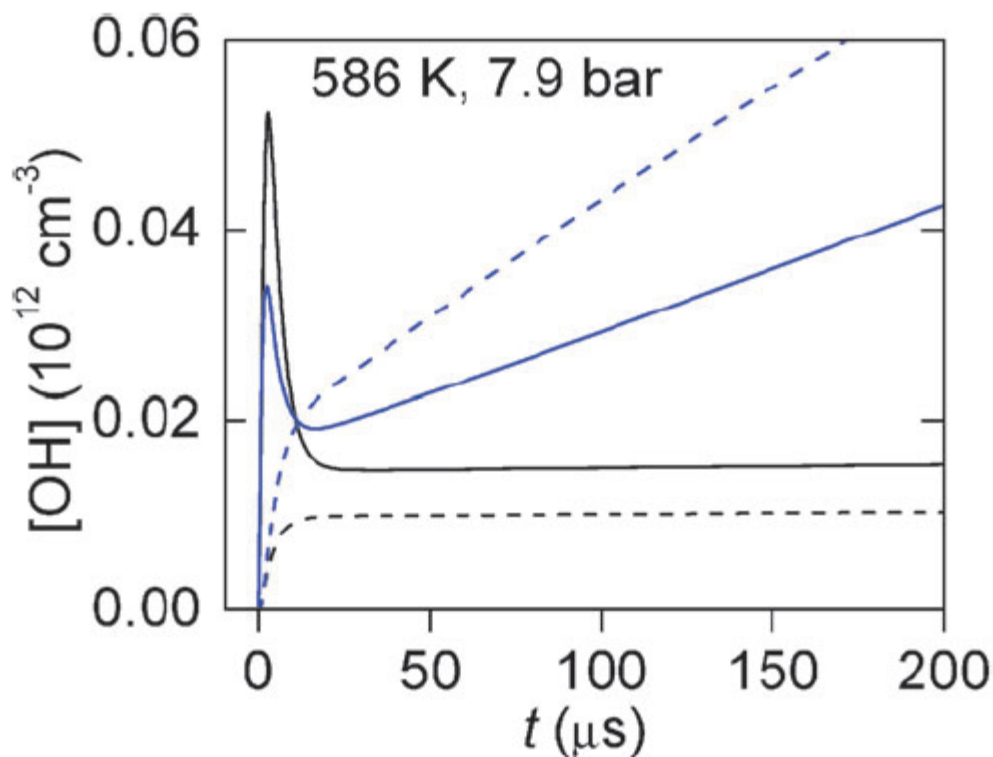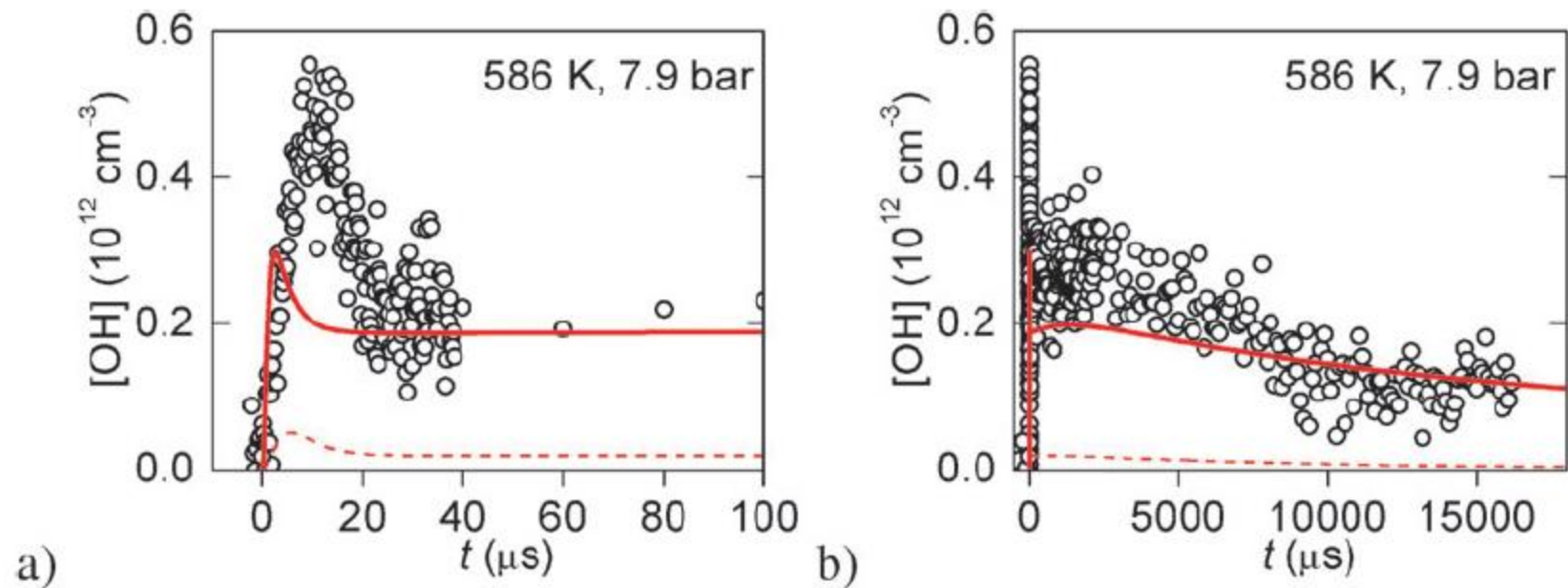

Fig. 5 Calculated OH concentration at 7.9 bar and 586 K using different models. The solid black line is the Knepp *et al.*[13] model; the dashed black line is the Knepp *et al.* model, but without formally direct pathways. The dashed blue line is the Silke *et al.*[41] mechanism, and the solid blue line is Silke *et al.* model, adding all rate coefficients from the ME calculation.

Effect of the chain branching on model calculations at (a)–(b) 586 K and (c) 828 K.

Evidence for chain branching at lower T
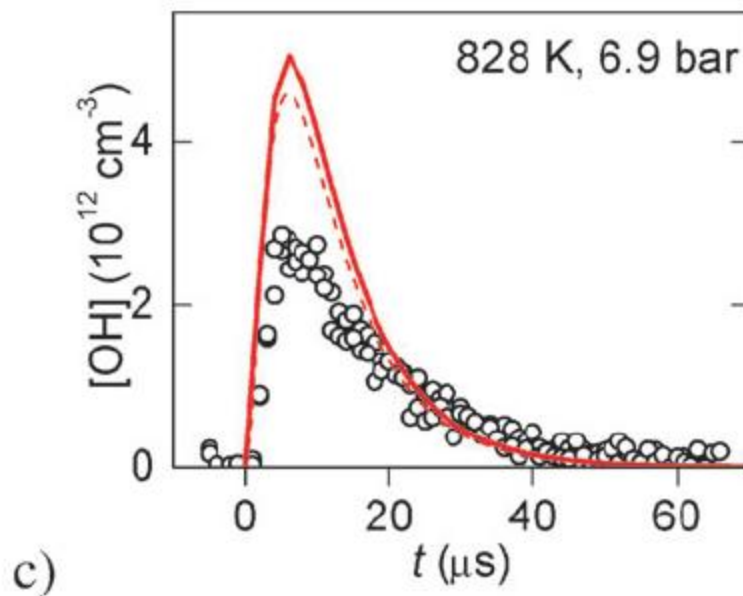
Direct observation of QOOH – difficult for dimethyl ether oxidation
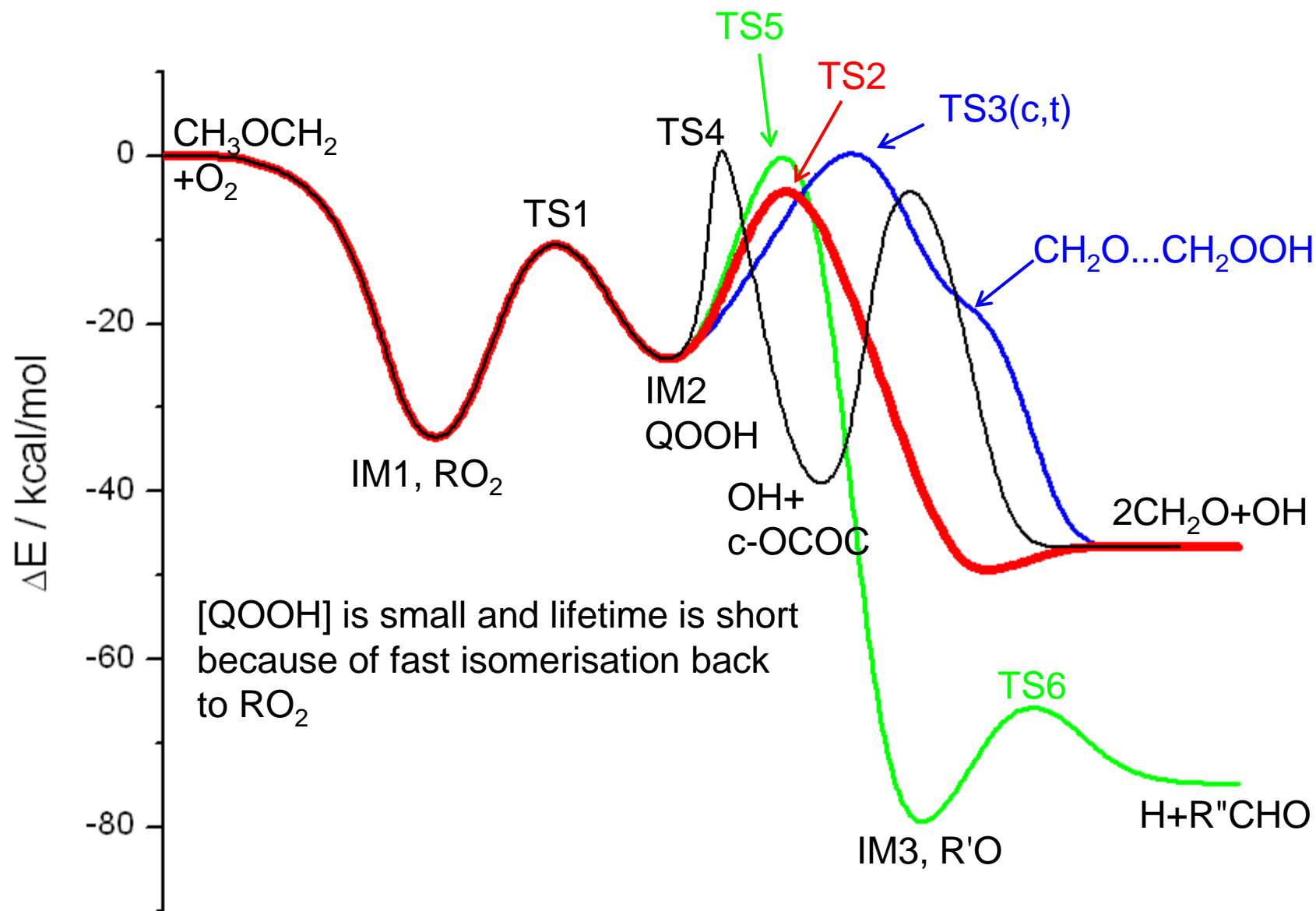
Direct observation of QOOH
Savee et al, Science, 2015, 346 (6222), p643

R = 2-butyl (red, derived from n-butane), 3-oxopent-2-yl (blue, derived from 3-pentanone) and 3,5-cycloheptadienyl (gray, Ra) and 2,4-cycloheptadienyl (black,Rb) (both derived from c-hpd and calculated in the present work).

Energy resolved mass spectra

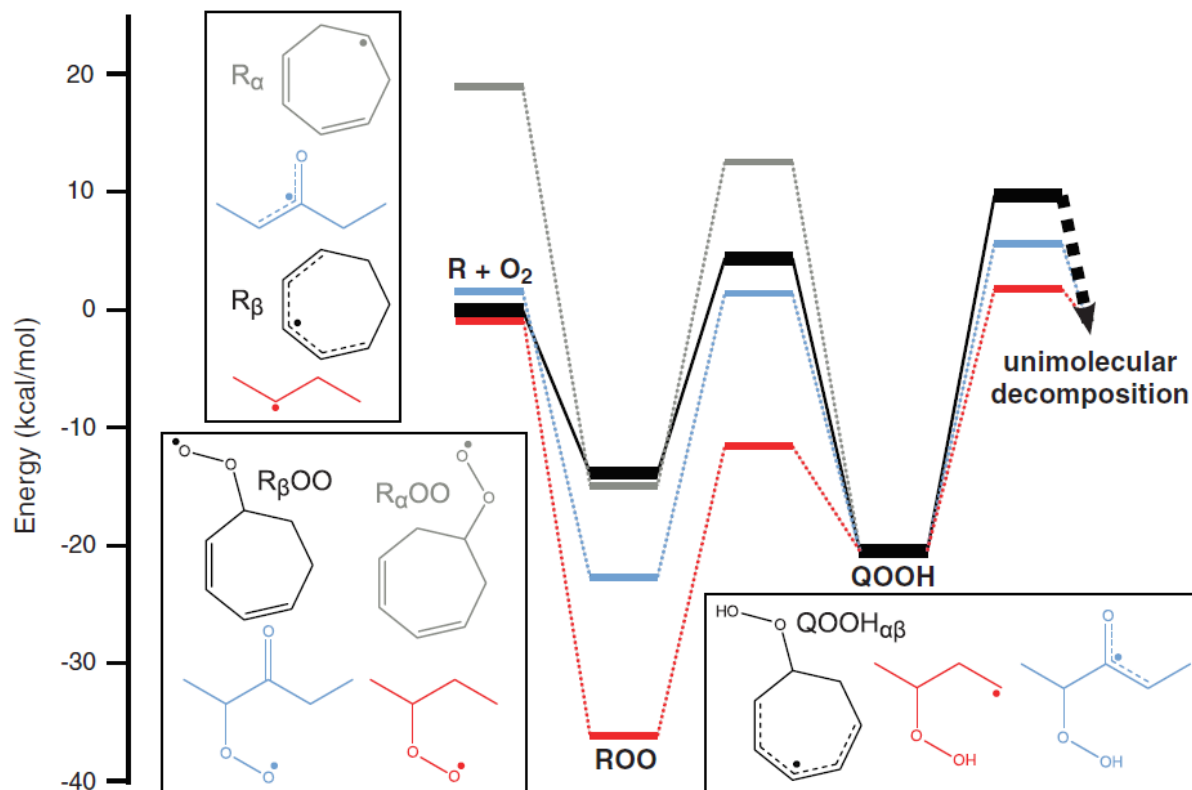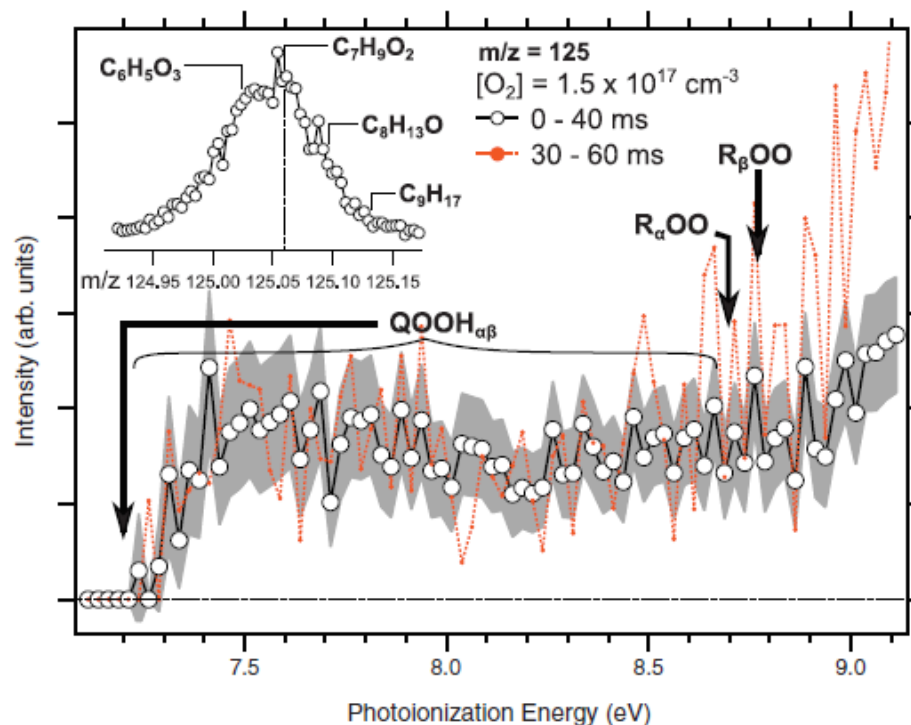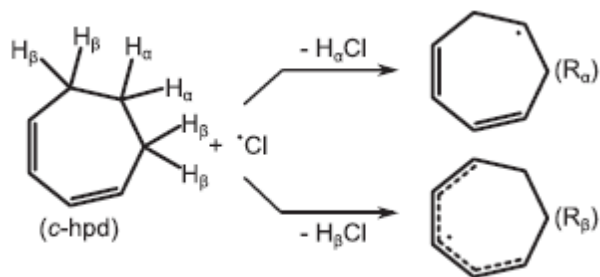- Above 8.5 eV, the spectrum depends on its observation time interval, suggesting the presence of at least two isomers consistent with $QOOH_{\alpha\beta}$ (AIE = 7.21 eV) and $R_\alpha OO$ (8.70 eV) and/or $R_\beta OO$ (8.78 eV). Calculated AIEs are marked by arrows.

QOOH kinetics

Rise:

$QOOH_{\alpha\beta} + O_2 \rightarrow$ Products

Decay:

$R_\beta + O_2 \rightarrow QOOH_{\alpha\beta}$
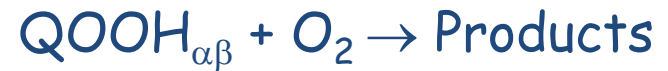
Remember $A \rightarrow B \rightarrow C$

$$b = \frac{a_0 k_1}{(k_2 - k_1)}\{\exp(-k_1 t) - \exp(-k_2 t)\}$$

Present case: $k_1 < k_2$
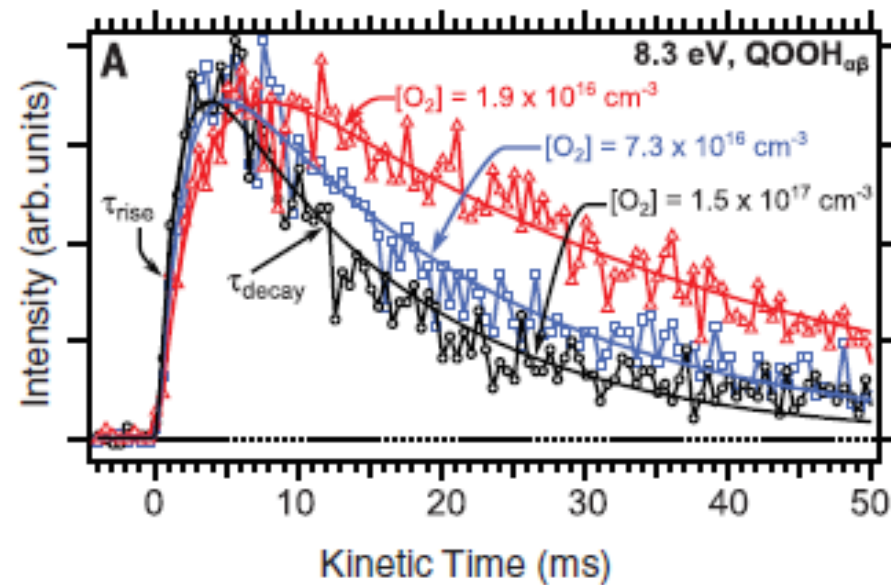
Peroxy radicals in atmospheric chemistry
Oxidation of volatile organic compounds (VOCs)

General oxidation scheme for VOCs

$$O_3 + h\nu \rightarrow O^1D + O_2$$
$$O^1D + H_2O \rightarrow 2OH$$
$$OH + RH\ (+O_2) \rightarrow RO_2 + H_2O$$
$$RO_2 + NO \rightarrow NO_2 + RO$$
$$RO \rightarrow\rightarrow HO_2\ (+R'CHO)$$
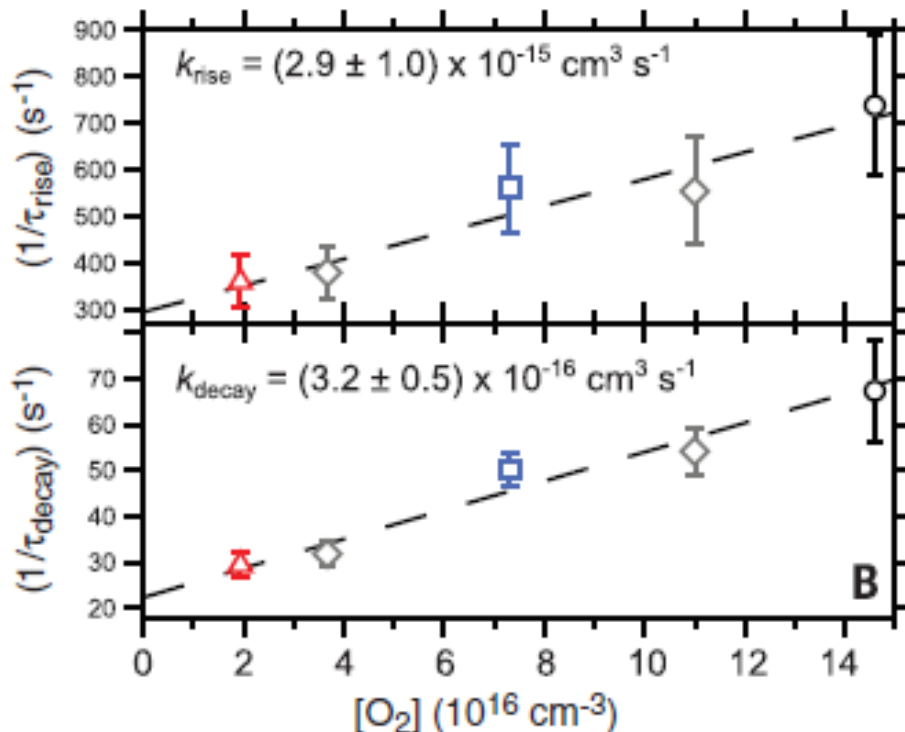$$HO_2 + NO \rightarrow OH + NO_2$$

$$NO_2 + h\nu \rightarrow NO + O;\ O + O_2 \rightarrow O_3$$

Secondary chemistry from R'CHO photolysis

Termination: $OH + NO_2 \rightarrow HNO_3$, $HO_2/RO_2 + HO_2/RO_2 \rightarrow$ Products. The termination route depends on the NO_x: VOC ratio

---

OVERALL
NO_x + VOC + sunlight → ozone
The same reactions can also lead to formation of secondary organic aerosol (SOA)

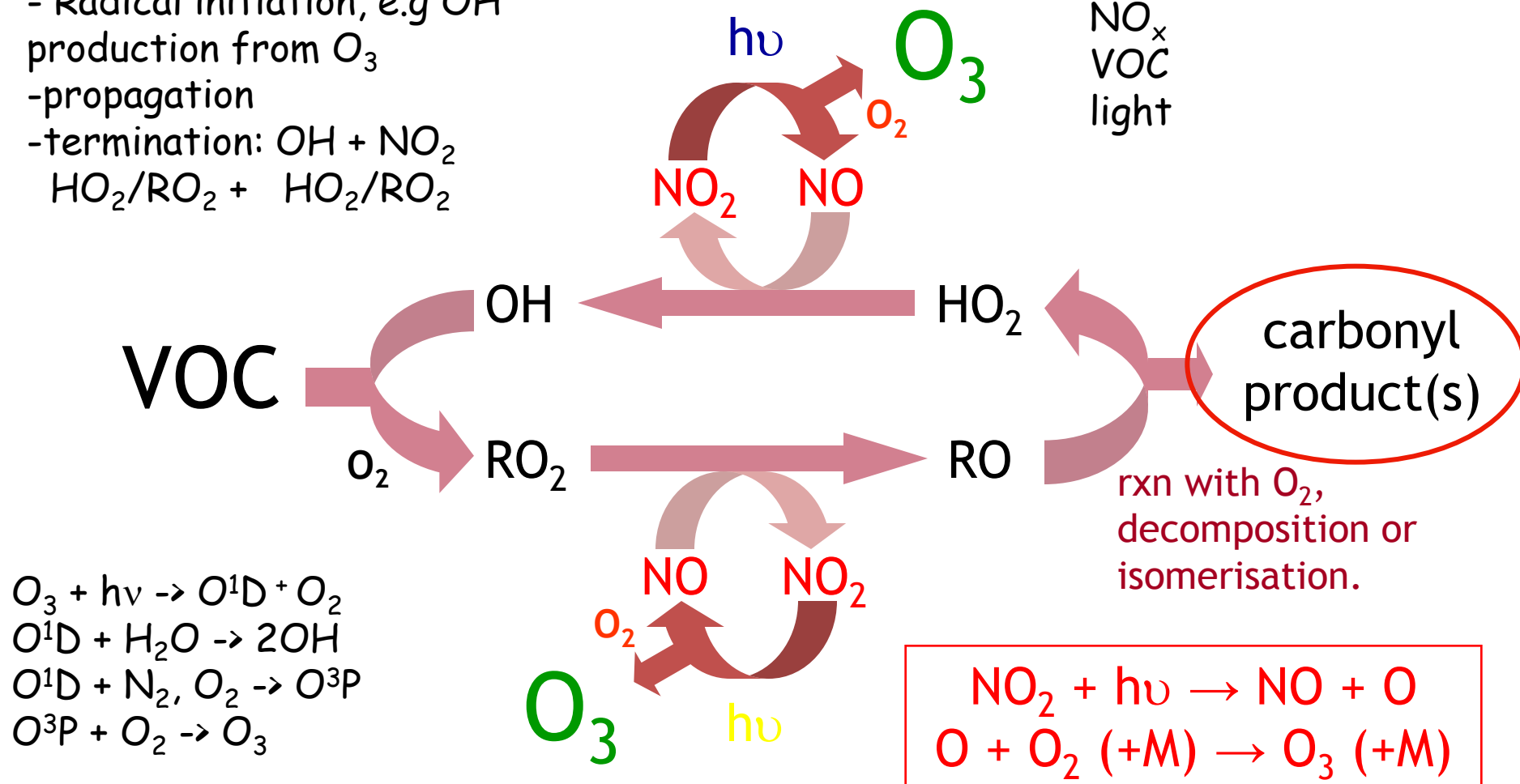# Free radical propagated oxidation cycle

Chain reaction:
- Radical initiation, e.g OH production from O_3
- propagation
- termination: $OH + NO_2$
  $HO_2/RO_2 + HO_2/RO_2$

Dependence on:
NO_x
VOC
light

$h\upsilon$ O_3 O_2

NO_2 NO

OH ← HO_2 carbonyl product(s)

VOC

O_2 RO_2 → RO

rxn with O_2, decomposition or isomerisation.

NO NO_2

O_2

O_3 $h\upsilon$

$O_3 + h\upsilon \rightarrow O^1D + O_2$
$O^1D + H_2O \rightarrow 2OH$
$O^1D + N_2, O_2 \rightarrow O^3P$
$O^3P + O_2 \rightarrow O_3$

$NO_2 + h\upsilon \rightarrow NO + O$
$O + O_2 (+M) \rightarrow O_3 (+M)$

Ozone formation from conversion of NO to NO_2

# Observations incompatible with conventional mechanism

- A number of recent field measurements in the Amazon, Pearl River Delta and Borneo found much higher concentrations of OH than conventional mechanisms predict.

- Measurements were made in regions with moderate to low concentrations of NOx high concentrations of the biogenic compound isoprene, C_5H_8.
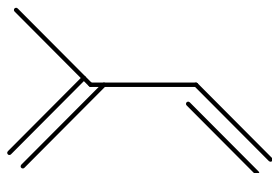
- This led to a focus on the chemistry of the peroxy radicals formed by reaction with O_2 and the radicals formed by OH addition to isoprene

Oxidation of isoprene in the atmosphere
Peeters et al
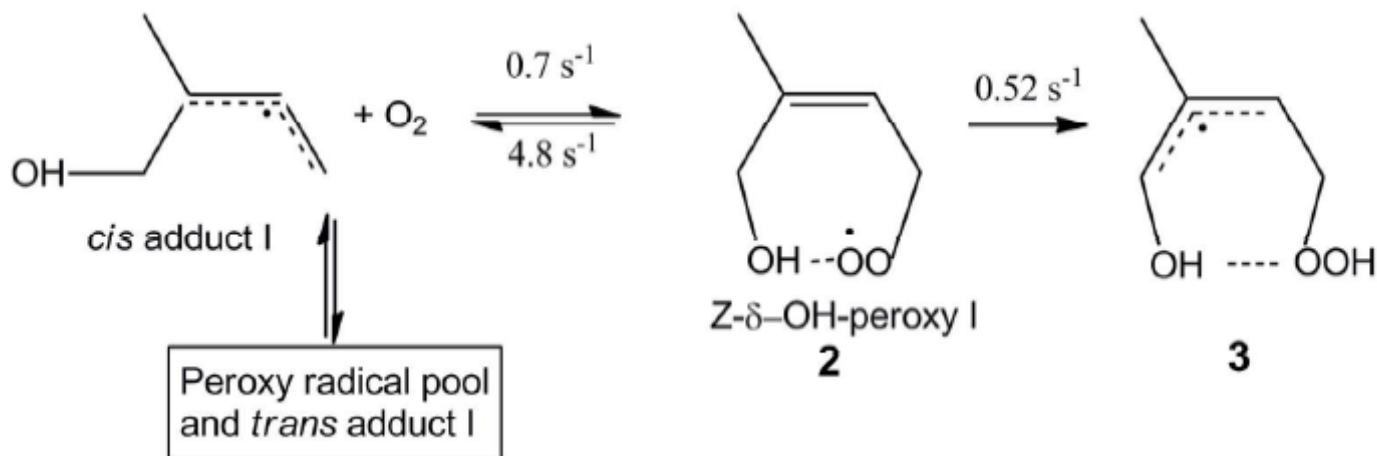
- OH adduct is an allylic radical, which is resonance stabilised. The peroxy radical formed from it is less stable than alkyl peroxy radicals (see earlier slide)

- As a result, the allylic QOOH is formed quite quickly.

- QOOH eliminates HO_2 to form $O=CHC(CH_3)=CHCH_2OOH$, which is photolysed to form OH and an oxy radical
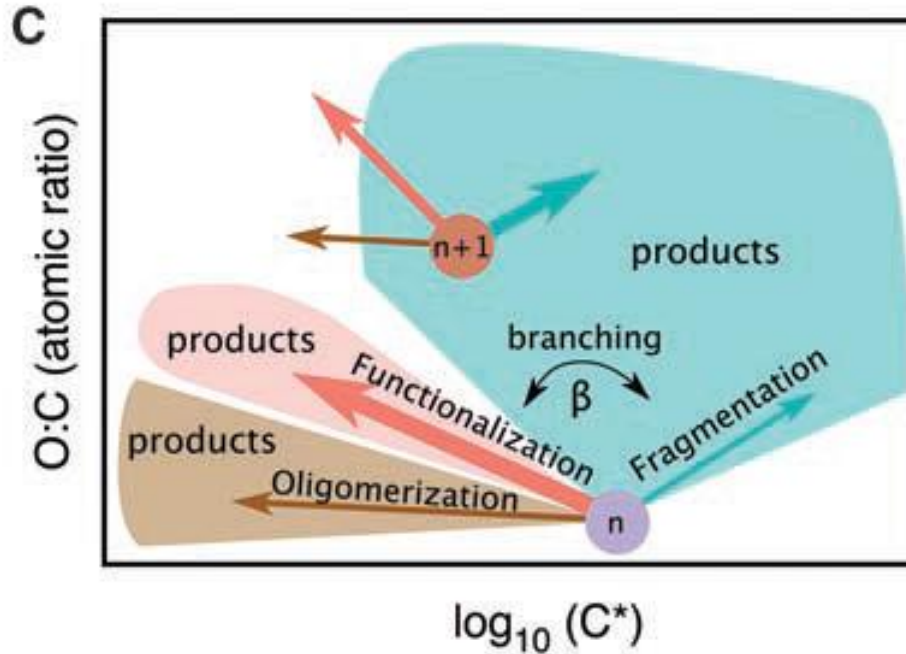
Composition of aerosol around the world – large contribution from organic compounds
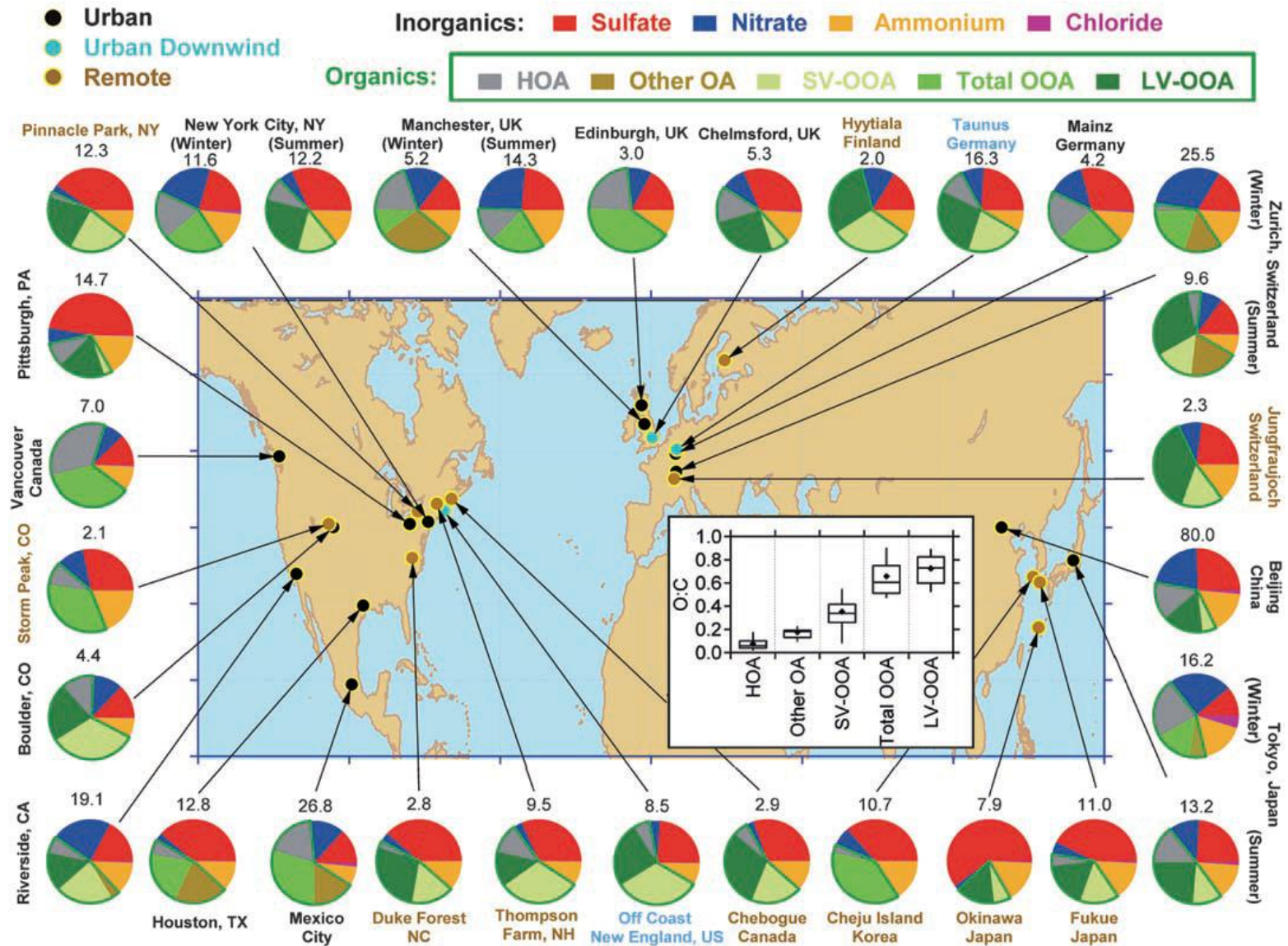
# Evolution of Organic Aerosols in the Atmosphere
Route to organic aerosols

Reactions form three categories: fragmentation, functionalization, or oligomerization, based on whether the carbon number decreases, stays the same, or increases. The figure shows the first two pathways. The branching ratio (β) between these pathways is critical. Functionalization will reduce volatility considerably, whereas fragmentation can generate more-volatile species, which are less likely to partition to the OA.

Riccobono et al. Science 2014, 344, 717

- Experimental evidence that highly oxidized compounds derived from biogenic emissions play an important role, in conjunction with sulphuric acid, in the formation of new particles in the boundary layer, requiring a mechanism in which the increased functionality occurs <u>rapidly</u>.

Autoxidation of aromatic compounds in the atmosphere
Crounse et al, J Phys Chem Lett 2013, 4, 3513
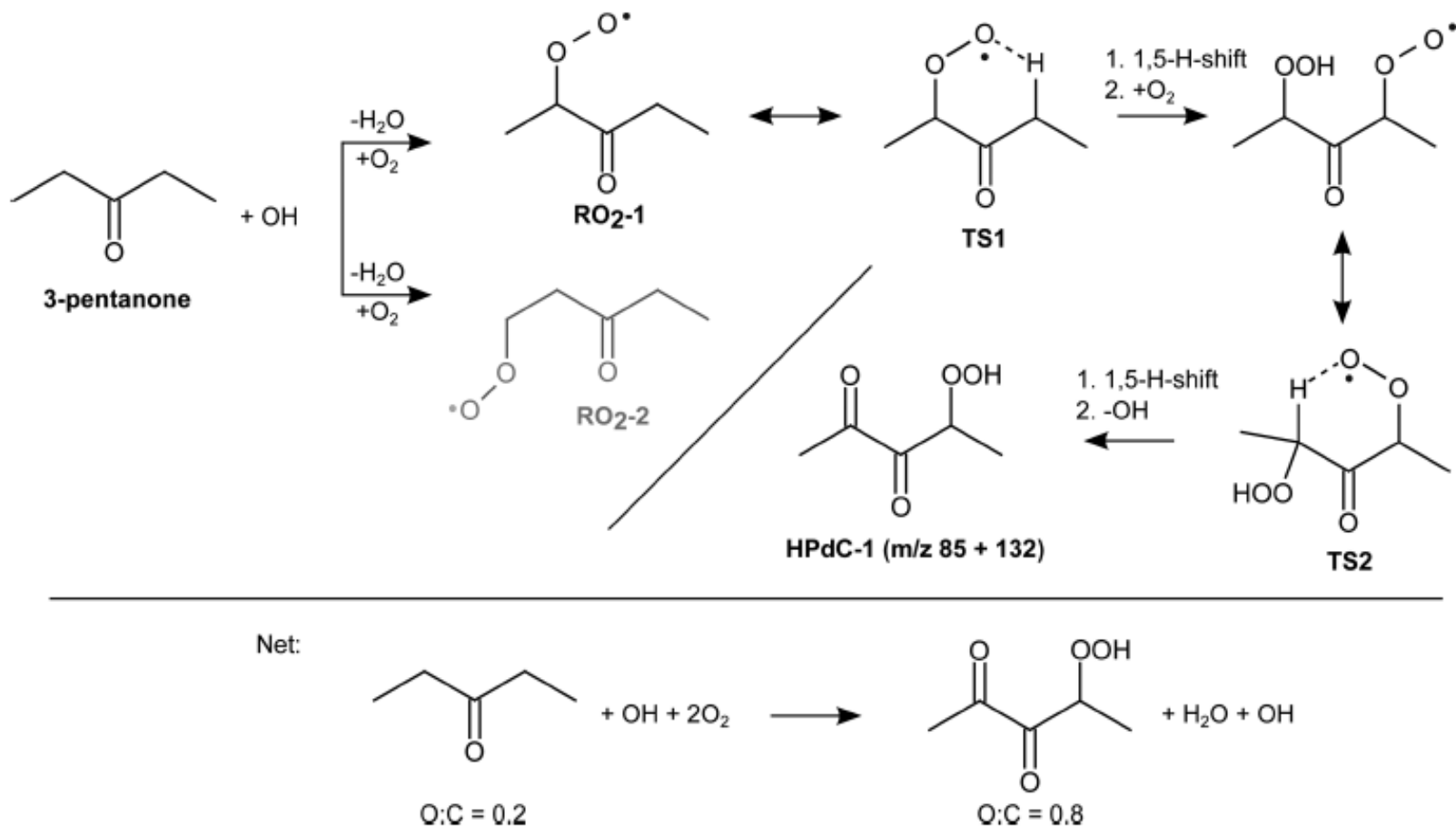
- A single cycle in the oxidation of 3-pentanone leads to a 4-fold increase in the O:C ratio